

# Journal of Advanced Pharmacy Research



## Section C: Drug Design, Delivery and Targeting

### Investigation of Therapeutic Potential of Nine Medicinal Plants Against Human Estrogen Receptor Alpha Enzymes: In Silico Study

Riswat Folashade Musbau<sup>1\*</sup>, Taiwo Hamidat Olaide<sup>2</sup>

<sup>1</sup>Department of Chemistry, University of North Dakota, Grand Forks, North Dakota, United States

<sup>2</sup>Department of Chemistry, School of Physical Sciences, Federal University of Technology, Akure, Ondo State, Nigeria

\*Corresponding author: Riswat Folashade Musbau, Department of Chemistry, University of North Dakota, Grand Forks, North Dakota, United States. Tel.: +17019794195

E-mail address: [riswat.musbau@und.edu](mailto:riswat.musbau@und.edu)

Submitted on: 31-08-2024; Revised on: 07-10-2024; Accepted on: 05-01-2025

To cite this article: Riswat Folashade Musbau, R. F.; Olaide, T. H. Investigation of Therapeutic Potential of Nine Medicinal Plants Against Human Estrogen Receptor Alpha Enzymes: In Silico Study. *J. Adv. Pharm. Res.* **2025**, 9 (1), 11-40. DOI: [10.21608/aprh.2025.317194.1289](https://doi.org/10.21608/aprh.2025.317194.1289)

#### ABSTRACT

**Objective:** Breast cancer remains the second leading cause of cancer-related deaths among women despite substantial research efforts and advancements in drug development, this study seeks to identify potent therapeutic compounds derived from nine medicinal plants for breast cancer by targeting the human estrogen receptor alpha enzyme (2IOG). **Methods:** A total of forty-three bioactive compounds were chosen from nine medicinal plants, such as *Annickia chlorantha*, *Allium sativum*, *Cyclopia genistoides*, *Rubus fruticosus*, *Brassica oleracea*, *Zingiber officinale*, *Camellia sinensis*, *Nigella sativa*, and *Linum usitatissimum*. Fulvestrant and Elacestrant served as control medications. The 3D structures of the ligands were obtained using the PubChem web server, and the crystal structure of 2IOG was accessed from the protein data bank. The SwissADME web server evaluated the virtual drug-likeness properties of the bioactive compounds, while AutoDock was used for molecular docking with 2IOG. The docked complexes were analyzed using the Proteins Plus and Protein-Ligand Interaction Profiler web servers, the bioactivity score was predicted using the Molinspiration web server, and the AdmetLAB 2.0 website was utilized to predict the ADMET characteristics of the ligands. **Results:** Among the screened compounds, four failed two or more of Lipinski's rules of five. The molecular docking analysis showed that twenty-one of the remaining thirty-nine bioactive compounds demonstrated higher binding energies against the protein target than the control drugs. Bioactive compounds such as Helichrysin, Epicatechin gallate, Catechin, Epicatechin, Gallic acid, Epigallocatechin, Chlorogenic acid, Naringenin, and Luteolin, showed favorable binding energies of (-7.5, -7.5, -8.2, -8.3, -8.5, -8.5 and -8.7) kcal/mol respectively. As opposed to Elacestrant and Fulvestrant which exhibited higher binding energies of (-6.3 and -6.7) kcal/mol respectively. Furthermore, these compounds demonstrate good bioactivity scores and excellent ADMET properties, highlighting their potential as promising candidates for further development. **Conclusion:** Therefore, these compounds, exhibiting favorable docking scores and effective interactions with the 2IOG protein, hold significant promise as strong potential candidates for developing breast cancer treatments. To confirm these computational findings, further research into their biological activity and laboratory studies such as molecular dynamics simulation, in-vivo and in-vitro are recommended.

**Keywords:** Breast cancer, In silico, Human estrogen receptor, Bioactive compounds, Drug-likeness, Molecular docking, Medicinal plant, 2IOG, ADMET.

## INTRODUCTION

Cancer is a globally lethal disease that greatly affects mortality rates, and currently, it has no cure. It is characterized by abnormal and uncontrolled cell division in the body, which spreads to various regions and damages tissues.<sup>1,2</sup> Cancer can impact any organ, including the lungs, kidneys, intestines, uterus, brain, and blood.<sup>3</sup> According to the World Health Organization (WHO), in 2018, there were 9.6 million cancer-related deaths, accounting for one in six fatalities, confirming cancer as the second leading cause of death worldwide.<sup>4</sup> Breast cancer, along with lung cancer, is among the most frequently diagnosed and deadliest forms of cancer, particularly affecting women with a high mortality rate. In 2011, it was the most prevalent and deadliest form of cancer.<sup>4,5</sup> Today, breast cancer continues to be the primary type of cancer diagnosed and is the second leading cause of cancer deaths in women globally.<sup>6</sup> The lower death rates seen in developing countries can be linked to advancements in mammographic screening and treatment options.<sup>7</sup> Elevated estrogen levels are known to increase breast cancer risk, influencing key processes such as initiation, malignant progression, and cell death by interacting with estrogen receptors found in breast cancer cells.<sup>8</sup>

There are two types of estrogen receptors: estrogen receptor alpha (ER $\alpha$ ) and estrogen receptor beta (ER $\beta$ ). However, ER $\beta$ 's role in cancer is not fully understood.<sup>9</sup> The genes encoding these two isoforms, ESR1 on chromosome 6 and ESR2 on a different chromosome, are responsible for regulating different gene sets. Both isoforms share a common structure featuring six functional domains labeled A through F.<sup>10</sup> They contain two activation functions: AF-1, which includes domains A and B, and AF-2, which encompasses domains E and F. The C domain serves as the DNA-binding region, while the D domain acts as a flexible hinge that contains the nuclear localization signal and connects the C and E domains. Meanwhile, the E domain contains the hormone-binding site.<sup>11</sup> Estrogen receptor alpha (ER- $\alpha$ ) is predominantly expressed in the uterus, vagina, mammary gland, liver, and pituitary gland.<sup>11</sup> An abnormal expression of estrogen receptor-positive is a primary factor in breast cancer, impacting around 70% of breast cancer patients. ER- $\alpha$  regulates the transcription of nuclear DNA necessary for mammary gland development and plays a key role in the signaling pathways associated with breast cancer. It also influences cell proliferation and differentiation through a paracrine mechanism. It is widely recognized that the range and location of estrogen receptors in breast tumors significantly affect clinical outcomes, with higher prognostic values greatly influencing patient survival rates.<sup>2,11</sup> Consequently, inhibiting estrogen receptors has emerged as a crucial

strategy in breast cancer prevention and treatment. Treatment methods often involve a combination of surgery, cytotoxic chemotherapy, radiation therapy, and targeted molecular endocrine therapy, depending on the specific type of breast cancer diagnosed.<sup>12</sup> Current drugs utilized in breast cancer treatment include Fulvestrant and Elacestrant, which are selective estrogen receptor degraders (SERDs).<sup>13</sup> Fulvestrant acts as a complete antagonist of the estrogen receptor, inhibiting its signaling through two mechanisms: it destabilizes the receptor by binding to it, preventing the formation of an open chromatin structure necessary for the transcription of ER-regulated genes.<sup>14,15</sup> Additionally, the ER-Fulvestrant and Elacestrant complex is unstable, leading to the breakdown of the ER protein through the ubiquitin-proteasome system.<sup>13,15</sup> These medications selectively bind to estrogen receptors, triggering both the activation of estrogen pathways (agonistic effects) and the inhibition of these pathways (antagonistic effects) in tissues with estrogen receptors. They may lead to side effects like blood clots, stroke, uterine cancer, or cataracts, as well as menopause-like symptoms such as hot flashes, night sweats, and vaginal dryness.<sup>11,15</sup> The adverse effects associated with these drugs highlight the need for the development of new and improved options. Due to the side effects of existing medications, we aimed to explore alternative and traditional methods to discover new drug compounds derived from various medicinal plants that are effective against breast cancer while remaining non-toxic to normal human cells.<sup>16</sup>

*Enantia chlorantha*, also known as *Annickia chlorantha* (Oliv.), belongs to the order Magnoliales and the family Annonaceae, and it is commonly called African yellow wood. This ornamental, dense forest tree is found throughout Sub-Saharan Africa, particularly in the eastern and southern forests of Cameroon, southern Gabon, Nigeria, Angola (Cabinda), Guinea, the Democratic Republic of Congo, Ivory Coast, and Liberia.<sup>17-19</sup> The *Annickia chlorantha* plant is known for its numerous pharmacological benefits, which include analgesic, antioxidant, anticonvulsive, antidiabetic, anti-inflammatory, antimicrobial, antimycobacterial, antiplasmodial, antipyretic, antisickling, antitumor, antiulcer, antiviral, hepatoprotective, hemostatic, testiculoprotective, and uterine stimulating properties.<sup>20</sup> Traditionally, different parts of this plant, such as the roots, stem, and bark, have been utilized to treat a variety of human health conditions, including anemia, bacterial infections, fevers, infected wounds, hepatitis, jaundice, leprosy, malaria, rickettsial fever, stomach pains, tuberculosis, typhoid fever, urinary tract infections, and yellow fever.<sup>19,21,22</sup>

*Allium sativum*, commonly known as garlic, is a bulb from the Liliaceae family, which includes around 600 species. Although it originated in Asia, garlic is now cultivated globally. Its medicinal use dates to ancient

times, with the Ebers papyrus noting its application in treating over 30 ailments.<sup>23,24</sup> Research indicates that garlic is effective in preventing and managing several conditions, including atherosclerosis, thanks to its ability to lower lipids, modestly reduce blood pressure, and exhibit fibrinolytic and anti-platelet properties. Additionally, garlic has antioxidant, hypotensive, antimicrobial, antifungal, antitumorigenic, and immunomodulatory effects.<sup>25</sup> Key to garlic's benefits are its organosulfur compounds, which help inhibit cancer development through mechanisms such as inducing apoptosis, stopping cell proliferation, scavenging reactive oxygen species (ROS), enhancing enzyme activity like glutathione-S-transferase, and decreasing tumor size. Studies have explored the impact of garlic-derived compounds on various cancer types.<sup>26,27</sup>

*Cyclopia genistoides* is a noteworthy medicinal plant known for its richness in mangiferin (MGF), which contributes to its numerous health benefits and is thought to play a key role in the bioactivity of Honeybush. This plant can be categorized into 20 species of flowering plants, including *C. intermedia*, *C. genistoides*, *C. maculata*, *C. sessiliflora*, and *C. longifolia*, all of which are native to the Cape Floristic Region of South Africa.<sup>28</sup> The leaves of Honeybush are often used to prepare medicinal beverages and herbal teas that are naturally caffeine-free and celebrated for their health advantages, including antioxidant, anti-mutagenic, and anti-carcinogenic properties.<sup>26-28</sup> Indigenous South Africans have utilized Honeybush tea for centuries in traditional medicine to address various health issues, such as respiratory infections, and digestive disorders, calming the central nervous system, and enhancing the immune response.<sup>29</sup> Additionally, it has been noted for its potential to help prevent skin cancer and to protect against oxidative stress through its radical scavenging abilities, iron-reducing effects, and inhibition of lipid peroxidation.<sup>28</sup>

*Rubus fruticosus*, commonly referred to as blackberry or European blackberry grows in North Africa, Brazil, and Europe. This species is prevalent in northern regions and has a longstanding history of use in traditional herbal medicine. Due to their potent antioxidant characteristics, European blackberry plants are utilized in herbal remedies for various applications, including antibacterial, anticancer, antidiarrheal, antidiabetic, and antidiarrheal purposes.<sup>30</sup> The blackberry plant (*R. fruticosus*) contains compounds such as tannins, gallic acid, villosin, and iron, while the fruit is rich in vitamin C, niacin (nicotinic acid), pectin, sugars, and anthocyanins, along with substances like albumin, citric acid, and malic acid.<sup>30</sup> Known for their medicinal properties, blackberries are particularly noted for their anticancer effects, as they help eliminate free radicals that can damage cells and potentially lead to cancer. Moreover, they enhance immune function, further reducing cancer risk, especially for cancers of the

esophagus, cervix, and breast. Traditionally, blackberry leaves have been used in herbal medicine for their antimicrobial effects and beneficial antioxidant properties.<sup>30</sup>

*Brassica oleracea*, commonly referred to as cabbage and belonging to the Brassicaceae family, has been a staple in human diets for centuries, both in fresh and preserved forms, as well as in vegetable oils and condiments.<sup>31</sup> Originating in the Eocene era in the Irano-Turanian region, the Brassicaceae family has since spread worldwide.<sup>32</sup> The Brassica genus encompasses various cruciferous vegetables, which are rich in essential minerals and vitamins including C, E, and K, along with folate and carotenoids like beta-carotene, lutein, and zeaxanthin. Additionally, these vegetables are an excellent source of fiber. Recently, interest in cruciferous vegetables has increased due to their potential anti-cancer properties, leading to research on the relationship between their consumption and cancer risk. Cruciferous vegetables contain glucosinolates, sulfur-containing compounds responsible for their distinctive taste and aroma.<sup>32</sup>

*Camellia sinensis*, commonly known as tea, is part of the Theaceae family and is predominantly grown in tropical and subtropical regions. It stands as one of the most widely consumed beverages globally and is a significant source of nutritional flavonoids.<sup>33</sup> Today, various types of tea are produced from the leaves of *Camellia sinensis* and are popular as a non-alcoholic alternative to water. These teas are classified based on their fermentation levels: green tea (unfermented), white and yellow teas (lightly fermented), oolong tea (semi-fermented), black tea (fermented), and puerh tea (post-fermented). Green tea contains caffeine along with antioxidant polyphenols; flavonoids in tea are noted for their beneficial effects, including anticarcinogenic, antimutagenic, antimicrobial, and antioxidant properties. It has been suggested to aid in various health issues, such as cancer prevention though this claim is primarily supported by limited epidemiological studies as well as cardiovascular diseases and AIDS.<sup>33</sup>

*Nigella sativa*, commonly known as black seeds or black cumin and belonging to the Ranunculaceae family, is valued for both its culinary uses and its long-standing role in traditional medicine. This plant is cultivated in various countries, including Egypt, Iran, Greece, Syria, Albania, Turkey, Saudi Arabia, India, and Pakistan. It is Indigenous to a vast region encompassing the eastern Mediterranean, northern Africa, the Indian subcontinent, and Southwest Asia.<sup>16,34</sup> Revered as a remedy, black cumin has been traditionally employed to address numerous health issues, such as rheumatism, asthma, bronchitis, headaches, back pain, anorexia, amenorrhea, paralysis, inflammation, mental weakness, eczema, and hypertension, among others. The extensive medicinal applications of *N. sativa* seeds are mainly due to their diverse therapeutic properties, which include

antioxidant, anti-inflammatory, immunomodulatory, anticancer, neuroprotective, antimicrobial, antihypertensive, cardioprotective, antidiabetic, gastroprotective, nephroprotective, and hepatoprotective effects.<sup>34</sup>

*Zingiber officinale*, commonly known as ginger, is a spice that originated in Southeast Asia and is extensively used to flavor foods and drinks. In addition, it has applications in traditional medicine to treat a range of ailments such as fever, digestive issues, arthritis, rheumatism, high blood pressure, and various infections, largely due to its anti-inflammatory, antioxidant, antimicrobial, and antiemetic effects.<sup>35</sup> Recent studies have also highlighted ginger extracts' significant chemopreventive effects against various types of cancer. Ginger contains over 60 active compounds, which can be categorized into volatile and nonvolatile types. These compounds have been researched for their antibacterial, antioxidant, and anti-inflammatory abilities, with ginger's phenolic compounds notably showing anti-tumor effects.<sup>36</sup>

*Linum usitatissimum*, commonly known as flaxseed, is a seed rich in oil and contains lignans, fiber, linoleic acid, alpha-linolenic acid, and various bioactive compounds that contribute to improved health. Flaxseed also referred to as linseed, is extensively cultivated globally, with Canada being the leading producer. Today, flaxseed is recognized as an exceptional functional food that offers numerous health benefits, including protection against cardiovascular disease, cancer, diabetes, dyslipidemia, obesity, and metabolic syndrome.<sup>37,38</sup>

Phytomedicine, which boasts over 2000 years of history, is the most ancient healthcare system, utilizing medicines derived solely from plants such as roots, bark, flowers, seeds, fruits, leaves, or branches. This practice is prevalent across many cultures, particularly in Asia, Africa, Europe, and America. Different types of herbal medicine originate from various cultures, each with unique preparation methods and treatment strategies.<sup>39</sup> Some herbs help combat cancer by enhancing the body's detoxification processes, while certain herbal derivatives and biological response modifiers inhibit cancer growth by affecting specific hormones and enzymes. Additionally, various phytoconstituents from medicinal plants are included in formulations designed to boost the immune system, leading to increased production of cytokines like interleukin, interferon, tumor necrosis factor, and colony-stimulating factor.<sup>40</sup>

The drug development process begins by identifying unmet medical needs, which arise from the inadequacy of existing diagnostic, therapeutic, and preventive methods. Following this, researchers identify biological targets suitable for drug development.<sup>41,42</sup> Discovering a new drug can be a lengthy and costly process; however, current strategies such as computer-

based techniques like docking, pharmacophore searches, and neural networking aim to minimize the time and costs associated with uncovering lead compounds that could potentially inhibit or modulate known drug targets. These computerized methods also help predict the metabolic pathways and pharmacokinetic profiles of drug molecules. Once a drug candidate is ready for the market, it's crucial to understand its absorption, distribution, metabolism, excretion, and toxicity (ADMET) profile.<sup>40</sup> Thus, assessing these characteristics early on can eliminate compounds with undesirable traits, ultimately reducing drug discovery costs.<sup>43</sup>

One strategy in the drug discovery process is the use of in-silico studies as a virtual screening method. This approach seeks to predict how molecular binders (ligands) interact with different molecules (protein targets) to create stable complexes. The in-silico method is frequently employed to discover new drugs, offering several advantages such as cost savings, time efficiency, and effectiveness.<sup>40</sup> Given the potential of the bioactive compounds in these plants for managing and treating breast cancer and other ailments, it is crucial to explore the drug-likeness, molecular docking, ADMET properties, and bioactivity properties approach to evaluate the inhibitory effects of certain bioactive compounds. Therefore, this study aims to investigate the inhibitory potential of *Annickia chlorantha*, *Allium sativum*, *Cyclopia genistoides*, *Rubus fruticosus*, *Brassica oleracea*, *Zingiber officinale*, *Camellia sinensis*, *Nigella sativa*, and *Linum usitatissimum* against human estrogen receptor  $\alpha$  using in-silico methods.

## MATERIAL AND METHODS

### LIGAND SELECTIONS

The study examines nine African plants: *Annickia chlorantha* (African Whitewood), *Allium sativum* (Garlic), *Cyclopia genitives* (Honeybush), *Rubus fruticosus* (Blackberry), *Brassica oleracea* (Cabbage), *Zingiber officinale* (Ginger), *Camellia sinensis* (Tea plant), *Nigella sativa* (Black cumin), and *Linum usitatissimum* (Flaxseed). A total of forty-three bioactive compounds were identified from these plants using various literature sources. The 2D structure of the bioactive compounds obtained from medicinal plants is depicted in **Figure 1-9**. From *Annickia chlorantha*, compounds such as Berberine, Palmatine, Jatrorrhizine, Caryophyllene oxide, and Spathulenol were selected. *Allium sativum* contributed Diallyl disulfide, Diallyl trisulfide, Allyl Mercaptan, and Gamma-glutamyl-S-2-propenyl. From *Cyclopia genistoides*, the compounds Helichrysin, Naringenin, 5,7,3,5-tetrahydroxyflavanone, Luteolin, and Isoliquiritigenin were identified. *Rubus fruticosus* provided Cyanidin-3-rutinoside, Cyanidin-3-xyloside, Quercetin, Chlorogenic acid, and Ellagic acid. *Brassica oleracea* supplied Lutein, Zeaxanthin,

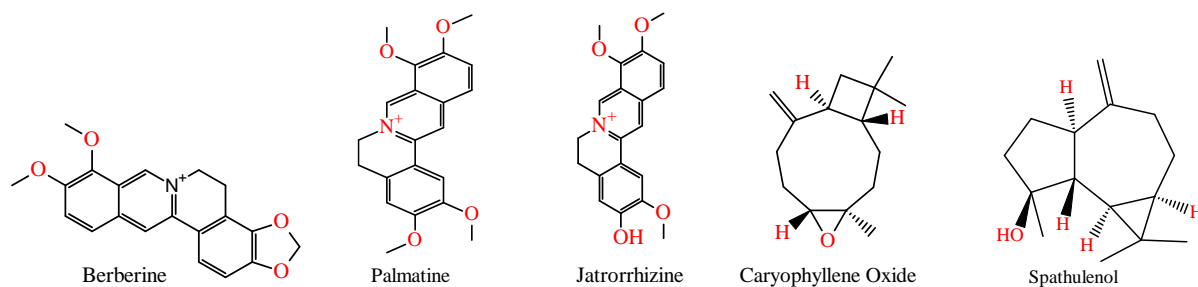


Figure 1. 2D structure of bioactive compounds from *Annickia chlorantha*

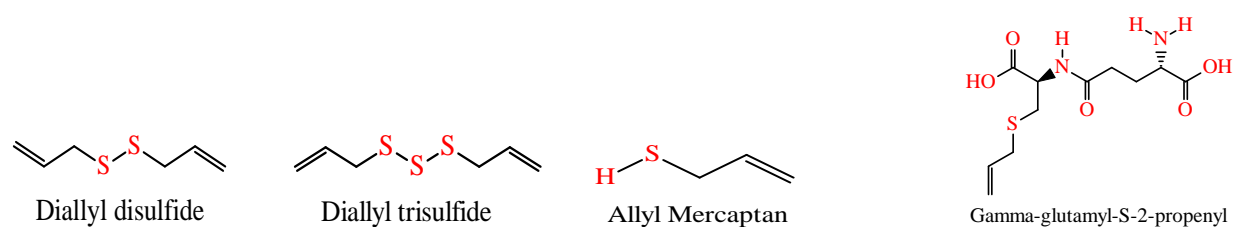


Figure 2. 2D structure of bioactive compounds from *Allium sativum*

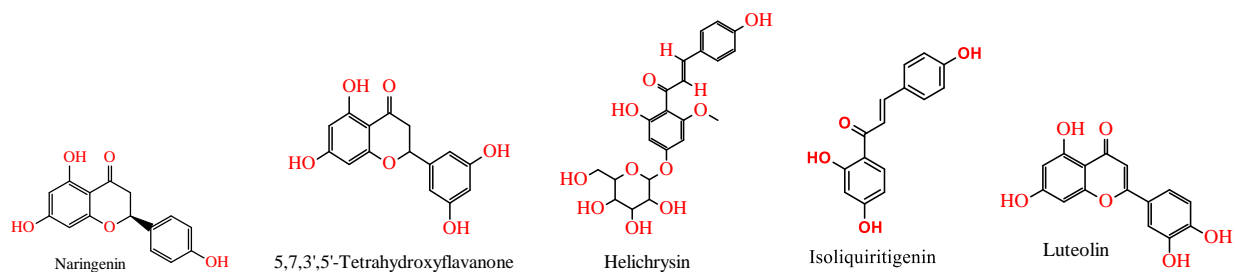


Figure 3. 2D structure of bioactive compounds from *Cyclopia genistoide*

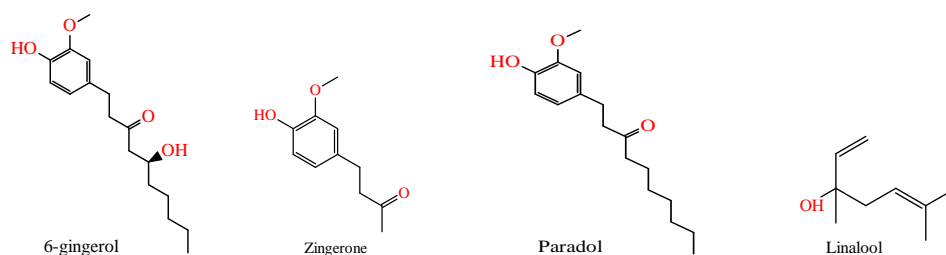


Figure 4. 2D structure of bioactive compounds from *Zingiber officinale*



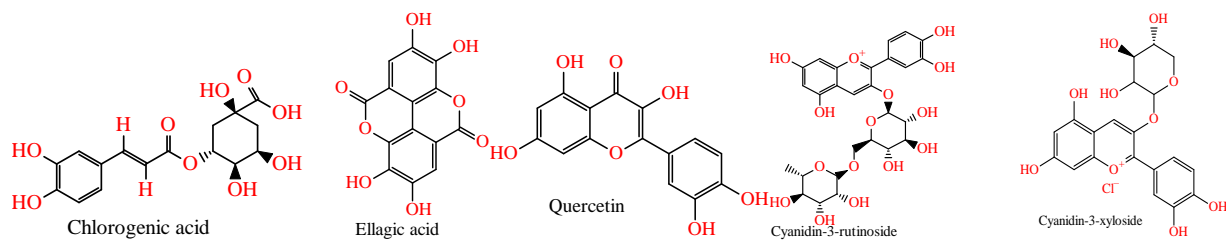


Figure 5. 2D structure of bioactive compounds from *Rubus fruticosus*

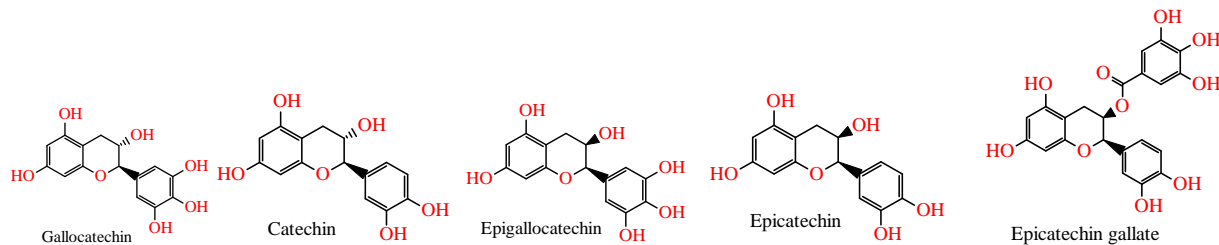


Figure 6. 2D structure of bioactive compounds from *Camellia sinensis*

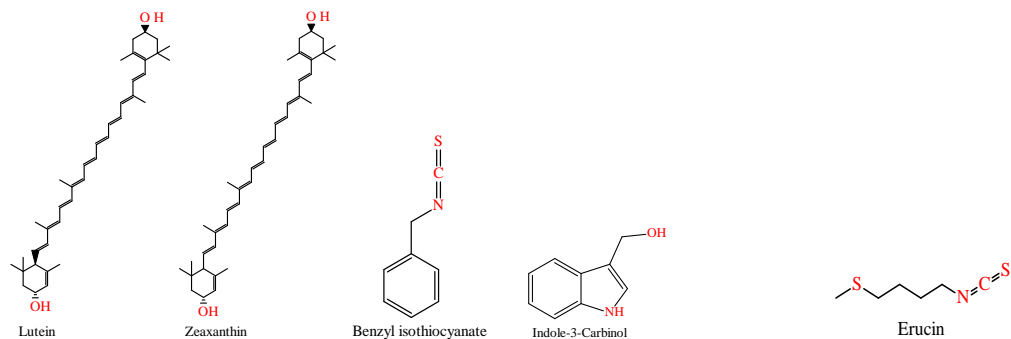


Figure 7: 2D structure of bioactive compounds from *Brassica oleracea*

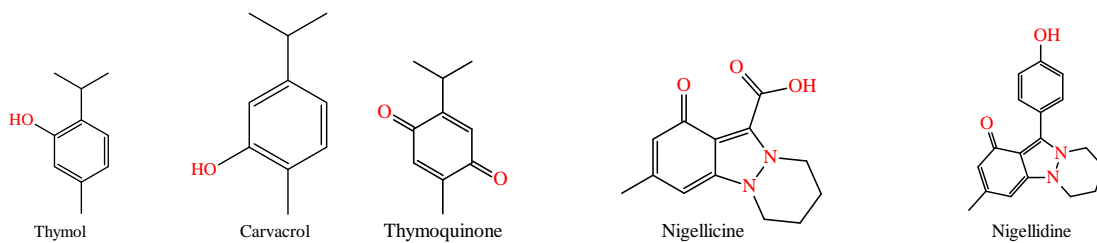


Figure 8. 2D structure of bioactive compounds from *Nigella sativa*

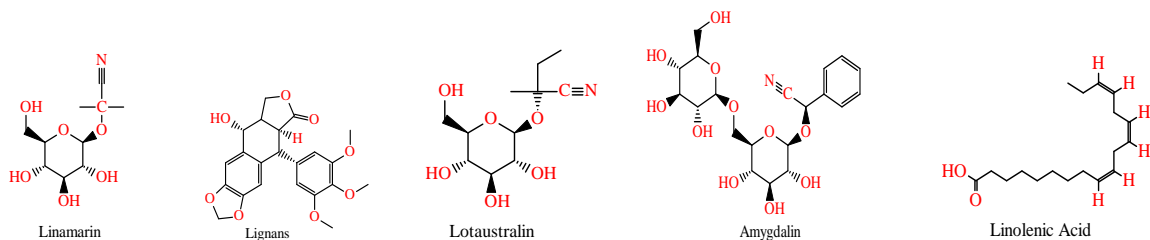


Figure 9. 2D structure of bioactive compounds from *Linum usitatissimum*

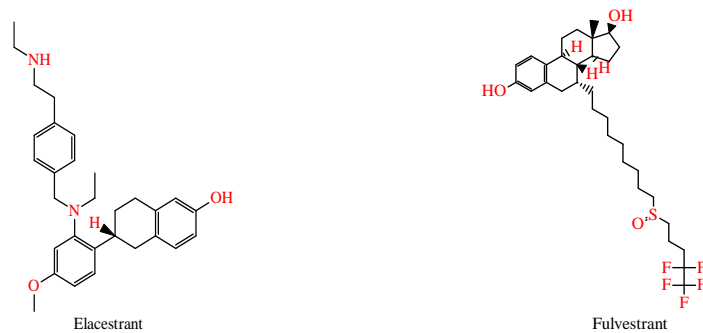


Figure 10. 2D structure of the Control drugs

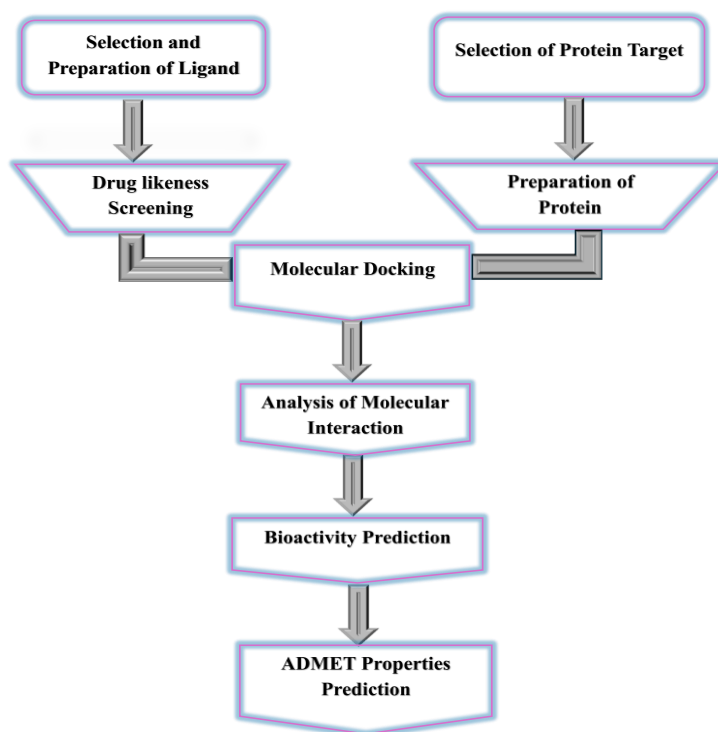


Figure 11. Flow chat of the study

Indole-3-carbinol, benzyl isothiocyanate, and Erucin. From *Zingiber officinale*, 6-gingerol, Paradols, Zingerone, and Linalool were selected. *Camellia sinensis*

contributed Gallic acid, Catechin, Epigallocatechin, Epicatechin, and Epicatechin gallate. *Nigella sativa* provided Thymol, Thymoquinone, Nigellidine,

Carvacrol, and Nigellidine, while *Linum usitatissimum* yielded Linamarin, Lignans, Linolenic acid, Amygdalin, and Lotaustralin. Fulvestrant and Elacencranstrant served as the control medications.<sup>13,23,28,29,31,34,36,37,44</sup> **Table 1** displays the bioactive compounds derived from the chosen plants and the control drugs utilized in this study. The online chemical database PubChem web (<https://pubchem.ncbi.nlm.nih.gov/>) was utilized to gather the PubChem identification number (PID), the 3D structures in structure data format (SDF), and the canonical SMILES for the bioactive compounds and the control drugs.<sup>45</sup>

### PROTEIN TARGETS SELECTION

The target protein associated with breast cancer is the Human Estrogen Receptor (2IOG). The three-dimensional (3D) crystallographic structure of this receptor, identified as PDB: 2IOG, in conjunction with the ligand N-[(1R)-3-(4-HYDROXYPHENYL)-1-METHYLPROPYL]-2-[2-PHENYL-6-(2-PIPERIDIN-1-YLETHOXY)-1H-INDOL-3-YL] ACETAMIDE (**11F**), can be found in existing literature. It was retrieved from the Research Collaboratory of Structural Bioinformatics (RCSB) Protein Data Bank ([RCSB PDB: Homepage](https://www.rcsb.org/)) and saved in PDB format.<sup>46,47</sup> **Figure 12** illustrates the structure of the human estrogen receptor alpha.

### PROTEIN TARGET PREPARATION

The three-dimensional structure of the target protein, Human Estrogen  $\alpha$  Receptor (2IOG), was refined and prepared by isolating it from co-crystallized ligands using UCSF-Chimera (version 1.13.1). This software removed non-inhibitors, added hydrogen atoms, and assigned Gasteiger-Huckel charges. The protein was then minimized for molecular docking and saved in PDB format.<sup>48</sup>

### DRUG LIKENESS VIRTUAL SCREENING

Virtual screening for the drug-likeness assessment of the forty-three bioactive compounds and two control drugs was performed using the SwissADME (<http://www.swissadme.ch/>) online server.<sup>49</sup> This process involved using the canonical SMILES notation for all the compounds and drugs involved. Four bioactive compounds did not adhere to two or more of the five Lipinski rules, while one control drug also failed to comply with one of these rules.<sup>50</sup> The other thirty-nine bioactive compounds and control drugs were subjected to molecular docking analysis.

### LIGAND OPTIMIZATION AND MOLECULAR DOCKING

Molecular docking of the ligands with the target protein was performed using PyRx software. The 3D structures of the downloaded ligands were uploaded sequentially into Open Babel, which is integrated within

PyRx. The ligands were then optimized to their lowest energy state for docking, utilizing the Merck molecular force field (MMFF94). Following this, the ligands were transformed into AutoDock ligand format (PDBQT). The docking studies between the ligands and protein receptors were conducted using AutoDock Vina, with a grid box centered at coordinates (x: 27.4179, y: 4.8911, z: 22.1521) and sized (x: 104.6134, y: 81.6814, z: 25.000 angstroms) to tailor the protein's active site. A total of thirty-six amino acids were selected from the literature as a binding region for the target protein and used in the molecular docking.<sup>51,52</sup> Exhaustion of 10 was implemented during the docking process. The binding energy, reported in kcal/mol, was calculated for each ligand-protein interaction. In addition, PyRx was used to convert the docked ligands and protein targets from PDBQT to PDB format, with the resulting files saved for further analysis and visualization.

### MOLECULAR INTERACTION ANALYSIS

The target protein and ligands were examined to create protein-ligand complexes utilizing the graphical user interface (GUI) software PyMOL, and these complexes were saved in PDB format. Afterward, the complexes were submitted to the Protein-Ligand Interaction Profiler (PLIP) webserver (<https://projects.biotec.tu-dresden.de/plip-web/plip/>) and the Proteins Plus web servers to analyze their 3D and 2D molecular interactions (<https://proteins.plus/>).<sup>20</sup>

### PREDICTION OF BIOACTIVITY SCORE

The bioactivity of the ligands was assessed using the online web server Molinspiration ([Molinspiration Cheminformatics](https://www.molinspiration.com/)) to calculate the biological activity scores for GPCR ligands, ion channel modulators, nuclear receptor ligands, kinase inhibitors, protease inhibitors, and enzyme inhibitors.<sup>53</sup> The following specific ranges were utilized to determine the bioactivity of the organic compounds: a compound is considered active if the bioactivity score is greater than 0 ( $> 0$ ), moderately active if the score falls between -5.0 and 0.0 ( $-5.0 \leq 0.0$ ), and inactive if the score is less than -5.0 ( $< -5.0$ ).

### PHARMACOKINETICS/ADMET PROPERTIES PREDICTION

The online tool ADMETlab (<https://admetmesh.scbdd.com/service/evaluation/cal>) was utilized to evaluate the absorption, distribution, metabolism, excretion, and toxicity (ADMET) properties of bioactive compounds identified through molecular docking. The compounds with superior binding scores than the control drugs were subjected to ADMET screening.<sup>54</sup>



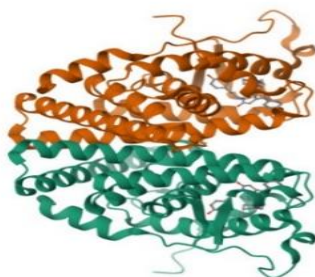


Figure 12. The crystal structure of Human estrogen receptor alpha (2IOG) ligand-binding in complex with compound 11F (Adopted from protein data bank).

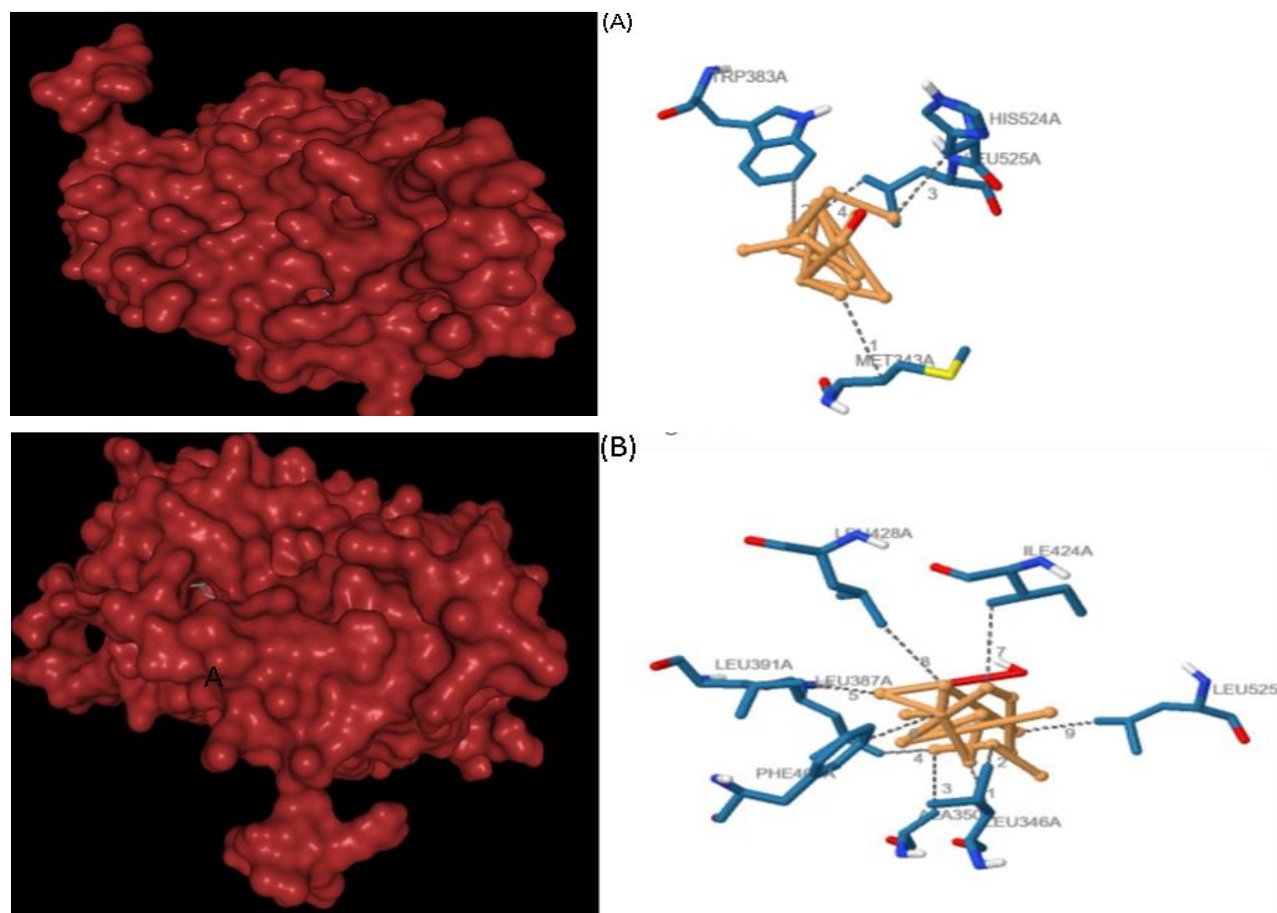
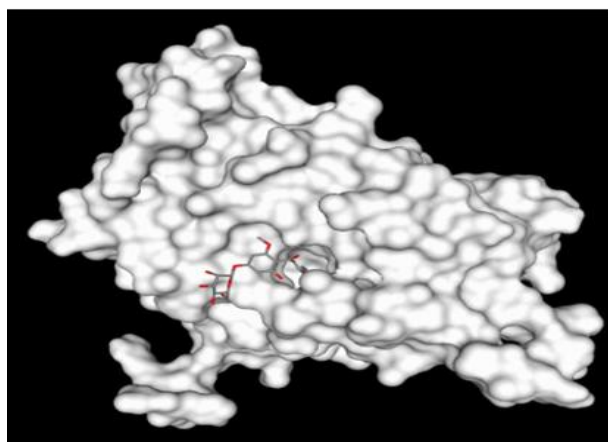
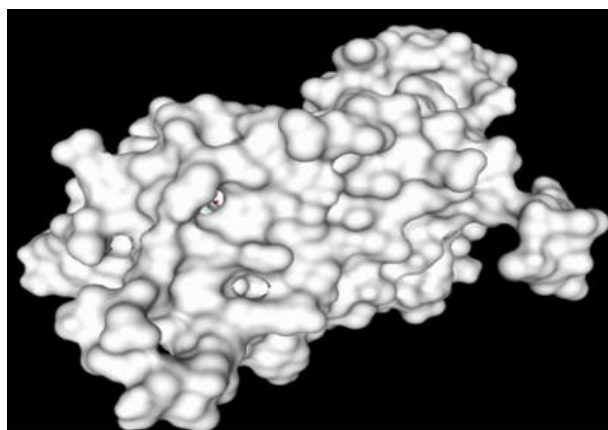
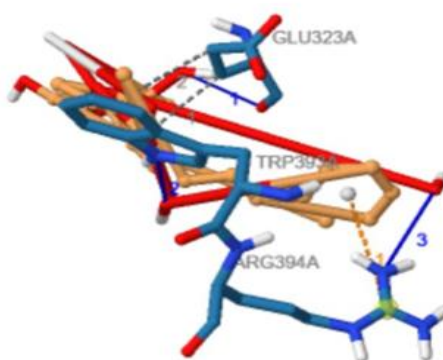


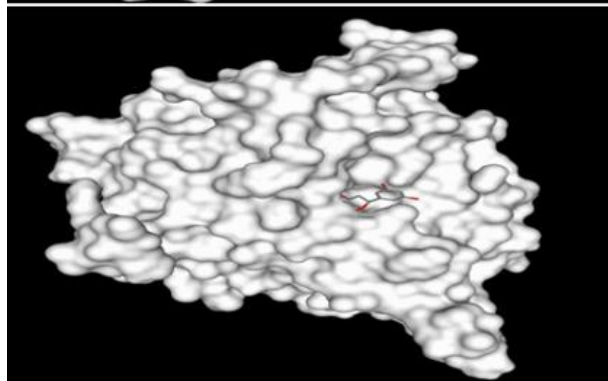
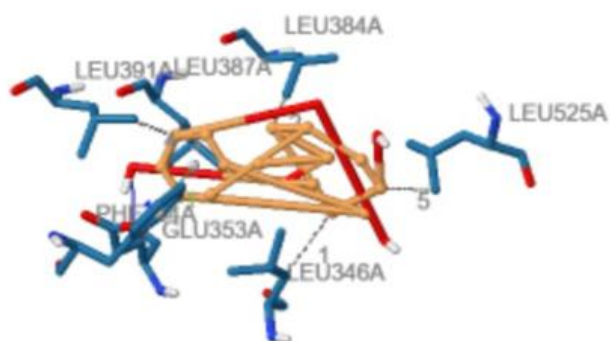
Figure 13. The binding arrangement of Caryophyllene oxide 13(a), and Spathulenol 13(b), within the active site of 2IOG, as determined through molecular docking using AutoDock.



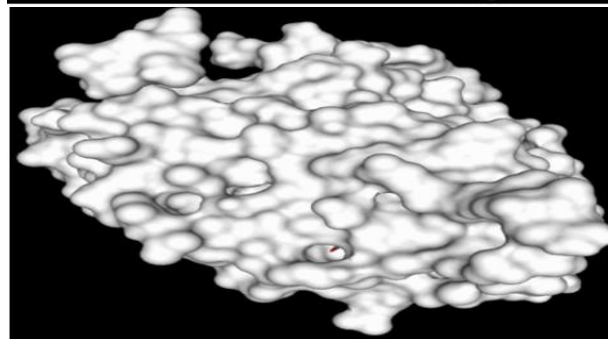
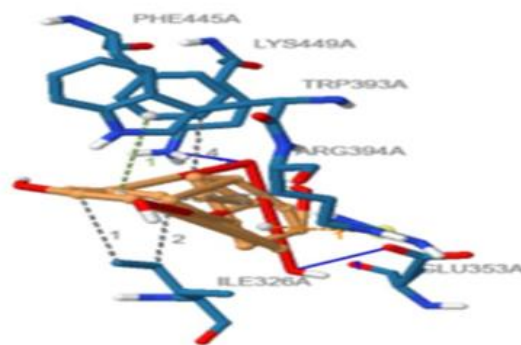
(A)



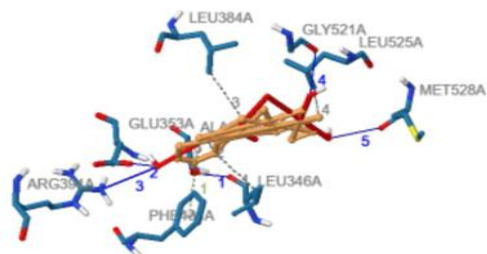
(B)



(C)



(D)



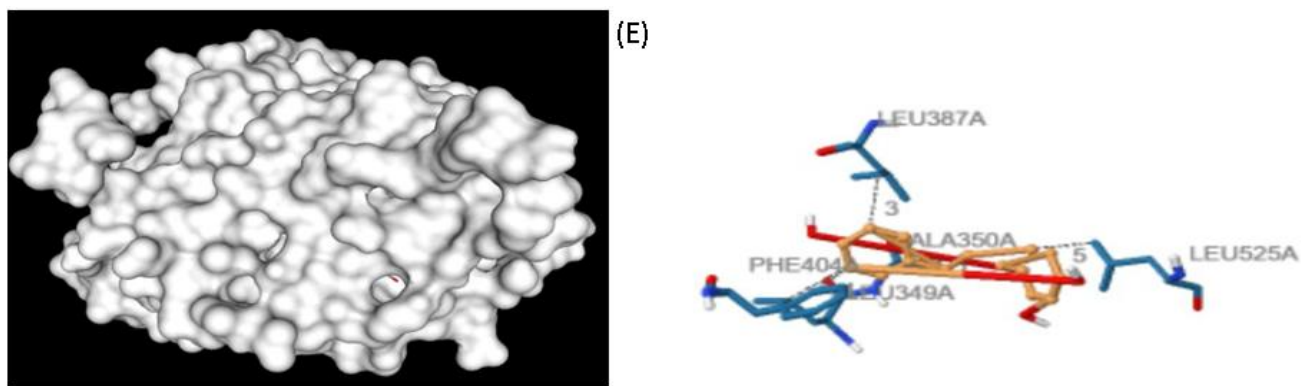
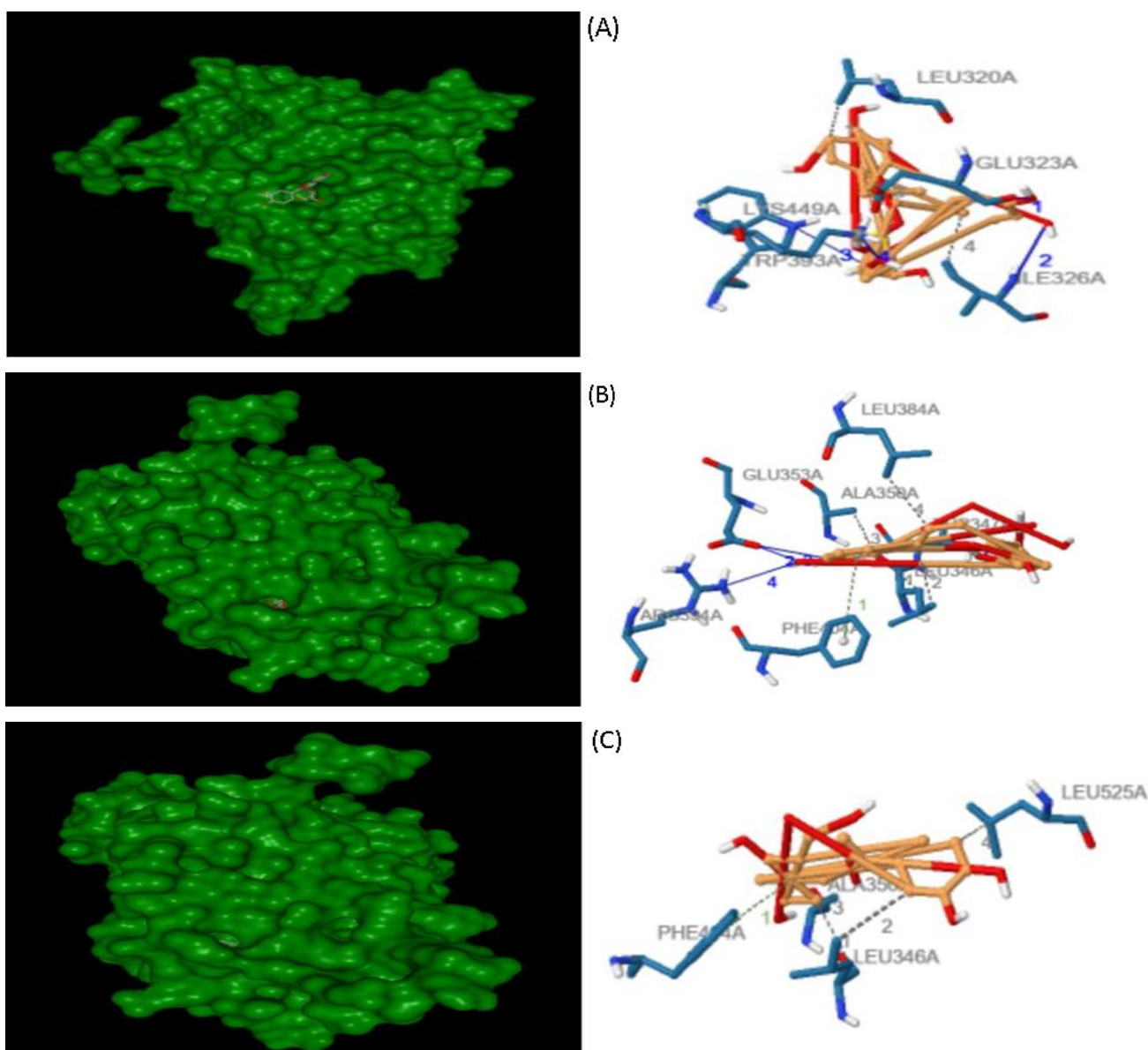


Figure 14. The binding arrangement of Helichrysin 14(a), Naringenin 14 (b), 5,7,3,5-tetrahydroxyflavanone 14 (c), Luteolin 14(d), and Isoliquiritigenin 14(e) within the active site of 2IOG, as determined through molecular docking using AutoDock.





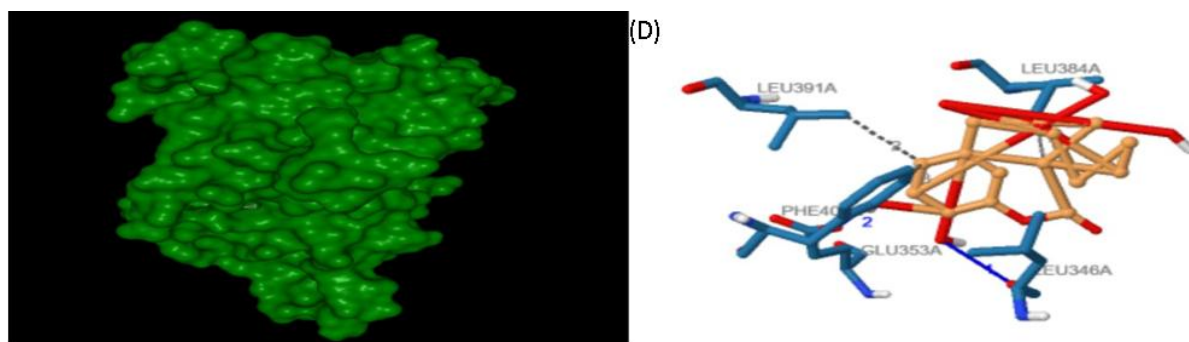
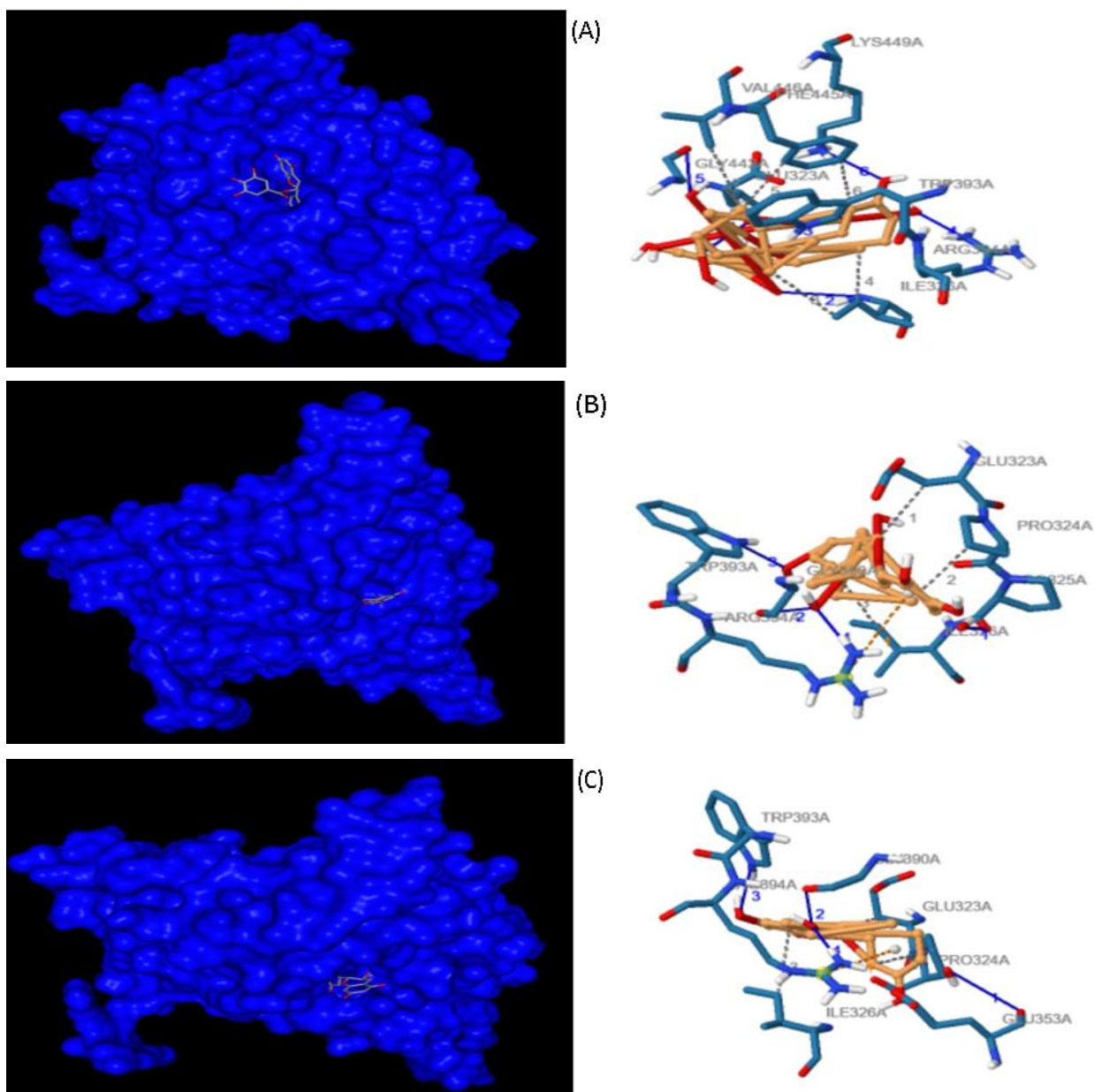


Figure 15. The binding arrangement of Cyanidin-3-xyloside 15(a), Chlorogenic acid 15(b), Quercetin 15(c), and Ellagic acid 15(d), within the active site of 2IOG, as determined through molecular docking using AutoDock



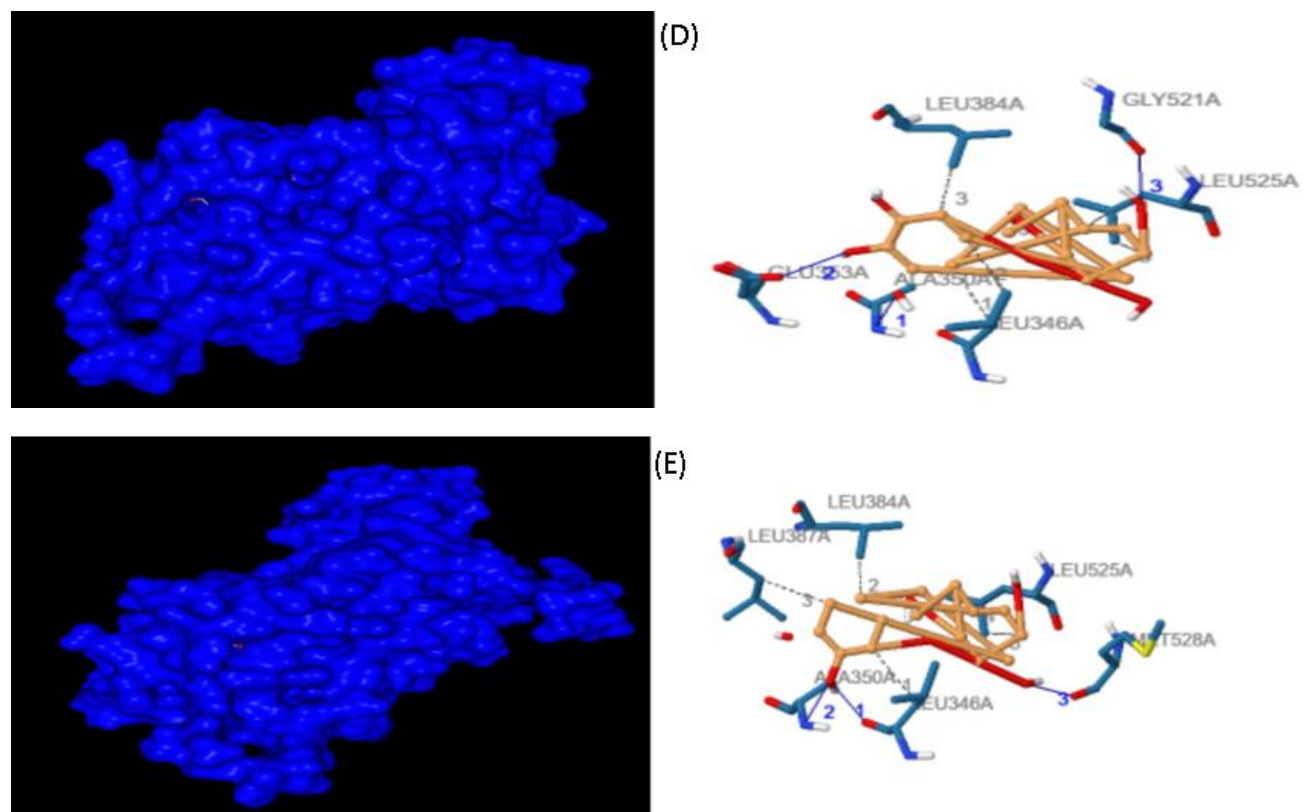


Figure 16. The binding arrangement of Epicatechin gallate 16(a), Gallicocatechin 16(b), Catechin 16(c), Epigallocatechin 16(d), and Epicatechin 16(e), within the active site of 2IOG, as determined through molecular docking using AutoDock.

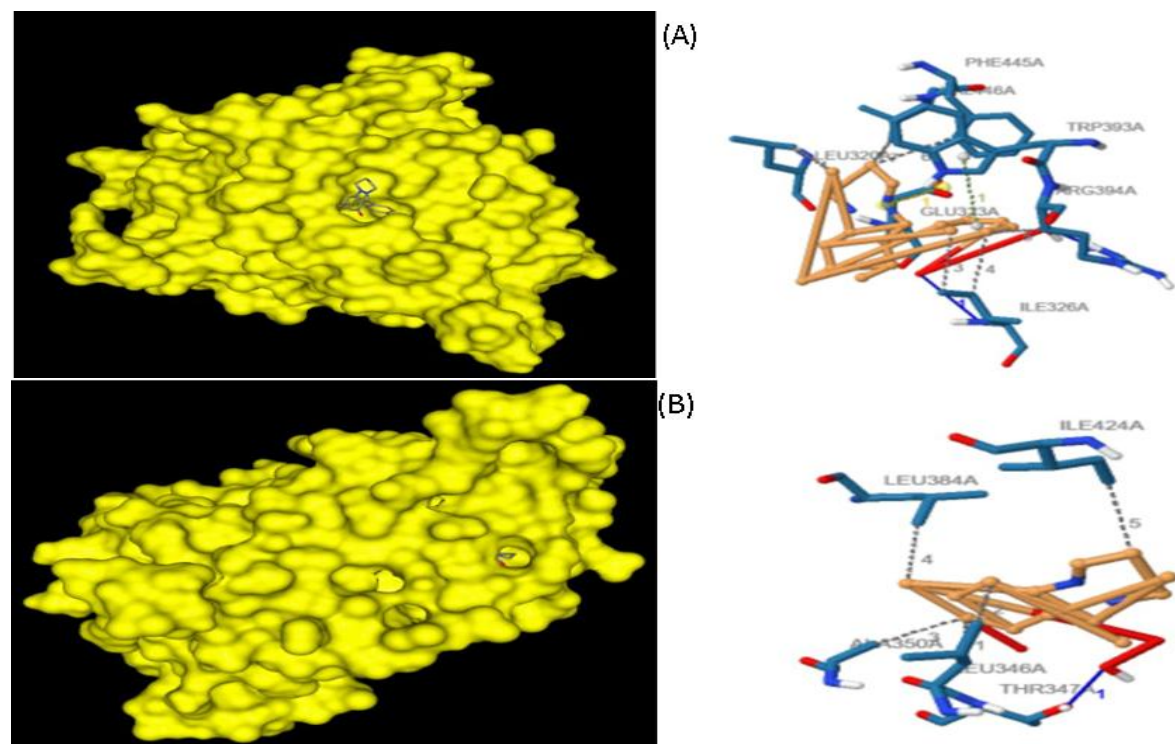


Figure 17. The binding arrangement of Nigellidine 17(a) and Nigellicine 17(b) within the active site of 2IOG, as determined through molecular docking using AutoDock.



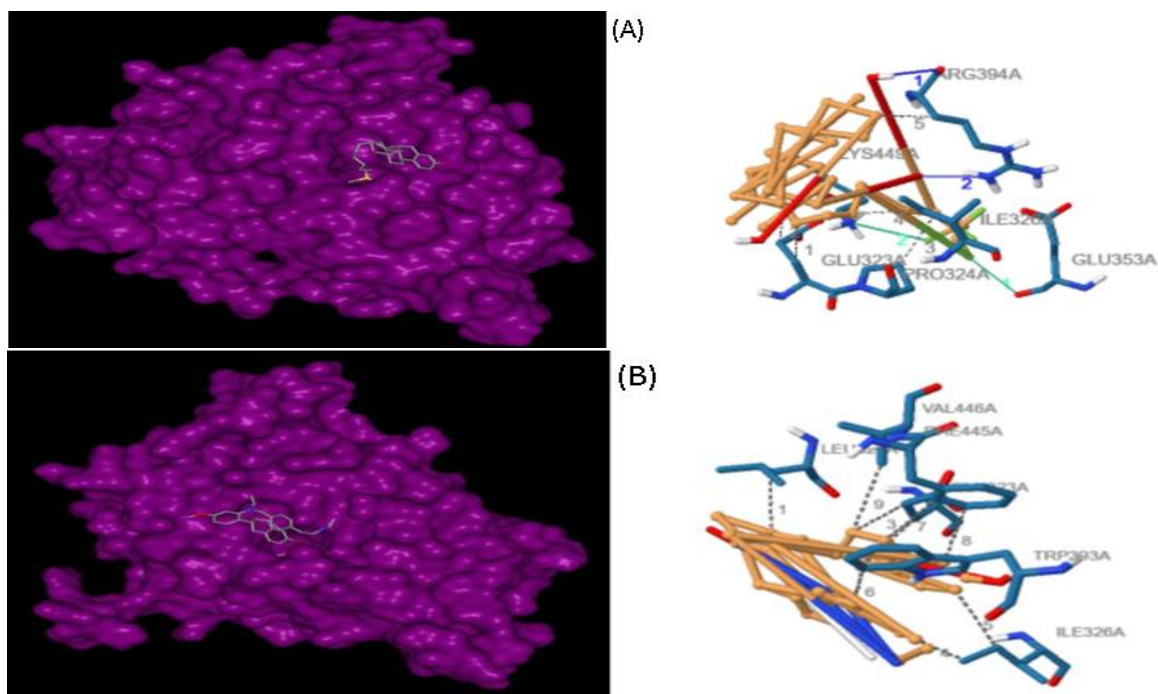


Figure 18. The binding arrangement of Fulvestrant 18(a) and Elacestrant 18(b) within the active site of 2IOG, as determined through molecular docking using AutoDock

## RESULTS

### DRUG LIKENESS SCREENING OF THE BIOACTIVE COMPOUNDS AND THE CONTROL DRUGS

Identifying the biological characteristics of prospective medications through drug-likeness screening is essential for the discovery and development of new pharmaceuticals. The SwissADME online tool was utilized to assess drug likeness. Drug-likeness results for bioactive compounds were gathered from nine African plants: *Annickia chlorantha*, *Allium sativum*, *Cyclopia genistoides*, *Rubus fruticosus*, *Brassica oleracea*, *Zingiber officinale*, *Camellia sinensis*, *Nigella sativa*, and *Linum usitatissimum*. Additionally, control drugs Fulvestrant and Elacestrant, used for breast cancer, were included in Table 1. The virtual screening revealed that four out of forty-three bioactive compounds (Amygdalin, Zeaxanthin, Lutein, and cyanidin-3-rutinoside) violated two or more of Lipinski's five rules and were excluded from further analysis. The other thirty-nine compounds that passed the rules, along with the two control drugs, were subjected to docking analysis with 2IOG.

### MOLECULAR DOCKING AND INTERACTION OF BIOACTIVE COMPOUNDS WITH HUMAN ESTROGEN RECEPTOR (2IOG)

The catalytic site of 2IOG contains thirty-six amino acid residues, specifically Met343, Leu346, Thr347, Leu349, Ala350, Asp351, Glu353, Leu354, Trp383, Leu384, Leu387, Met388, Leu391, Arg394, Phe404, Val418, Glu419, Gly420, Met421, Ile424, Phe425, Leu428, Gly521, His524, Leu525, Tyr526, Met528, Lys529, Cys530, Lys531, Asn532, Val533, Val534, Pro535, Leu536, and Leu539<sup>51,55</sup>. This study utilized auto dock vina tools for molecular docking analysis to assess the binding efficiency, electrostatic energy, hydrophobic interactions,  $\pi$ -stacking interactions,  $\pi$ -cation interactions, salt bridges, and hydrogen bond interactions between bioactive compounds and the human estrogen receptor alpha (2IOG). The data presented in **Table 2** below illustrates the potential biological activity of bioactive compounds extracted from nine African plants against the target protein, 2IOG, along with their estimated binding energy score.

The bioactive compounds in *Annickia chlorantha* are Palmatine, Berberine, Jatrorrhizine, Spathulenol, and Caryophyllene oxide showing binding energies of (-6.1, -6.2, -6.6, -7.9, and -8.1) kcal/mol respectively with the target protein 2IOG. The molecular interactions and binding of Caryophyllene oxide and Spathulenol with human estrogen receptor (2IOG) are depicted in **Figures 13 a-b**. Caryophyllene oxide forms 4 hydrogen bonds with GLU323, ILE326, TRP393, and

LYS449. Additionally, it exhibits hydrophobic interactions with LEU320, GLU323, and ILE326, along with an interaction with LYS449. Caryophyllene oxide does not have any  $\pi$ -stacking interaction. Spathulenol demonstrates 9 hydrophobic interactions with LEU346, ALA350, LEU387, LEU391, PHE404, ILE424, LEU428, and LEU525 without any interaction with hydrogen bonds or  $\pi$ -stacking.

The bioactive compounds in *Cyclopia genistoides*; Helichrysin, 5,7,3,5-tetrahydroxyflavanone, Naringenin, and Isoliquiritigenin, luteolin, bind to 2IOG with binding energies of (-7.5, -7.6, -8.1, -8.5, and -8.7) kcal/mol respectively. **Figures 14 a-e** show the molecular interaction and binding of these 5 bioactive compounds with the 2IOG protein. Helichrysin establishes 3 hydrogen bonds with GLU323, TRP393, and ARG394, 2 hydrophobic interactions with GLU323, and 1  $\pi$ -cation interaction with ARG394. Naringenin demonstrates 5 hydrophobic interactions with LEU346, LEU384, LEU387, LEU391, and LEU525, 1 hydrogen interaction with GLU353, and 1  $\pi$ -stacking with PHE404. 5,7,3,5-tetrahydroxyflavanone interacts hydrophobically with ILE326, ARG394, and PHE445. It also forms a hydrogen bond with GLU353 and LYS449, along with  $\pi$ -stacking with TRP393 and  $\pi$ -cation with ARG394. Luteolin demonstrates 5 hydrogen bonds with LEU346, GLU353, ARG394, GLY521, and MET528, interacts hydrophobically with LEU346, ALA350, LEU384, and LEU525, and forms  $\pi$ -stacking with PHE404. Isoliquiritigenin interacts with LEU349, ALA350, LEU387, PHE404, and LEU525 using hydrophobic interactions and does not establish any interaction with hydrogen bonds,  $\pi$ -cation, or  $\pi$ -stacking. The bioactive compounds present in *Rubus fruticosus* are Cyanidin-3-xyloside, Chlorogenic acid, Ellagic acid, and Quercetin. The molecular interaction of these bioactive substances with the target protein (2IOG) is shown in **Figure 15 a-b**; they give binding energies of (-7.0, -8.1, -8.4, and -8.5) kcal/mol respectively. Cyanidin-3-xyloside forms 4 hydrogen bonds with GLU323, ILE326, TRP393, and LYS449, along with 3 hydrophobic interactions with GLU323, PRO324, and ILE326, and 1 salt bridge with LYS449. Quercetin establishes bonds with LEU346, ALA350, and LEU525 using hydrophobic interaction, as well as a  $\pi$ -stacking interaction with PHE404. Chlorogenic acid interacts with THR347, GLU353, and ARG394 using hydrogen bonds, demonstrates hydrophobic interaction with LEU346, ALA350, and LEU384, and establishes  $\pi$ -stacking with PHE404. Ellagic acid forms 2 hydrogen bonds with LEU346 and GLU353 and demonstrates 3 hydrophobic interactions with LEU384, LEU391, and PHE404.

The following bioactive compounds Erucin, benzyl isothiocyanate, and Indole-3-carbinol found in *Brassica oleracea* bind to the target protein with binding energies of (-2.6, -5.1, -6.2) kcal/mol. However, none of

the bioactive compounds has a binding energy higher than the control drugs. Hence, they were eliminated from additional analysis.

Linalool, Paradols, Zingerone, and 6-gingerol, are the bioactive substances present in *Zingiber officinale*. The molecular docking of these compounds with the 2IOG protein target gives binding energies of (-5.6, -6.0, -6.2, -6.4) kcal/mol respectively. The binding energy values are lower in comparison with the drug control, so they were not visualized for 3D and 2D interaction.

**Figure 16 a-e** illustrates the interaction of the target protein with the bioactive compounds present in *Camellia sinensis*. Epicatechin gallate, Catechin, Gallocatechin, Epicatechin, and Epigallocatechin exhibit binding energies of (-7.5, 8.2, -8, -8.2, -8.2, and -8.3) kcal/mol respectively, with the 2IOG in the molecular docking results. Gallocatechin bonds hydrophobically with GLU323, PRO324, and ILE326. It also forms hydrogen bonds with PRO325, GLY390, TRP393, and ARG394, along with establishing a  $\pi$ -cation interaction with ARG394. Catechin establishes 4 hydrogen bonds with GLU353, GLY390, TRP393, and ARG394. Additionally, it forms 3 hydrophobic interactions with GLU323, PRO324, and ILE326, and  $\pi$ -stacking with ARG394. Epigallocatechin interacts with hydrogen bonds in three different ways: ALA350, GLU353, and GLY521, and exhibits hydrophobic interactions with LEU346, LEU384, and LEU525. Epicatechin forms hydrogen bonds with LEU346, ALA350, and MET528, and demonstrates hydrophobic interactions with LEU346, LEU384, LEU387, and LEU525. Epicatechin gallate demonstrates 6 hydrogen bonds with GLU323, ILE326, TRP393, ARG394, GLY442, and LYS449. Additionally, it forms 5 hydrophobic interactions with GLU323, ILE326, PHE445, and VAL446.

The bioactive compounds present in *Nigella sativa*, including Thymol, Thymoquinone, Carvacrol, Nigellidine, and Nigellicine, exhibit binding energies of (-6, -6, -6.2 -6.9, and -7.7) kcal/mol, respectively, when interacting with the protein target in molecular docking. (**Figure 17 a-b**) shows that Nigellicine establishes hydrophobic interactions with LEU346, ALA350, LEU384, and ILE424. It also forms a hydrogen bond with THR347. Nigellidine demonstrates hydrogen bonds with ILE326 and ARG394. Additionally, it hydrophobically interacts with LEU320, GLU323, ILE326, ARG394, PHE445, and VAL446. The  $\pi$ -stacking interaction is with TRP393, while the salt bridge is with GLU323.

The bioactive compounds in *Allium sativum*, namely Allyl mercaptan, Diallyl disulfide, Diallyl trisulfide, and Gamma-glutamyl-S-2-propenyl, exhibit binding energies of (-2.7, -3.9, -3.8, and -5.8) kcal/mol respectively, with the 2IOG protein. Linamarin, Lignans, linolenic acid, and Lotaustralin are the identified bioactive compounds found in *Linum usitatissimum*.

They have binding energies of (-4.7, -5.9, and -6.3) kcal/mol respectively, with the 2IOG protein in the molecular docking results. However, all the bioactive compounds found in both *Allium sativum* and *Linum usitatissimum* were eliminated before further analysis because they exhibited higher binding energies than the control drugs.

Elacestrant and Fulvestrant which served as control drugs exhibited binding energies of (-6.3 and -6.7) kcal/mol respectively, with the target protein, indicating effective interaction during molecular docking (**Figure 18 a-b**). Fulvestrant interacts with halogen bonds GLU352 and LYS449, hydrogen bonds with ARG394, as well as hydrophobic interactions with GLU323, PRO324, ILE326, and ARG394. Meanwhile, LEU320, GLU323, ILE326, TRP393, PHE445, and VAL446 interact hydrophobically with Elacestrant.

### BIOACTIVITY PREDICTION

The bioactivity properties of the bioactive compounds with greater binding energies than the control drugs are shown in **Table 3**. This bioactivity includes scores for GPCR ligands, ion channel modulators, nuclear receptor ligands, kinase inhibitors, protease inhibitors, and enzyme inhibitors. For the GPCR ligands, Jatrorrhizine, Caryophyllene oxide, Spathulenol, Luteolin, Isoliquiritigen, Cyanidin-3-xyloside, Quercetin, Ellagic acid, and Nigellidine have scores between -5.0 and 0.0, indicating they are moderately active. In contrast, 5,7,3',5'-Tetrahydroxyflavanone, Helichrysin, Naringenin, Chlorogenic acid, 6-gingerol, Gallic acid, Catechin, Epigallocatechin, Epicatechin, Epicatechin gallate, Nigellidine, Lignans, Elacestrant, and Fulvestrant have scores greater than 0.0, indicating that they are active. The ion channel modulator scores of Spathulenol, 5,7,3',5'-Tetrahydroxyflavanone, Naringenin, Luteolin, Isoliquiritigen, Cyanidin-3-xyloside, Quercetin, Ellagic acid, Nigellidine, Lignans, and Fulvestrant range from -5.0 to 0.0, indicating they are moderately active. In contrast, the scores of Jatrorrhizine, Caryophyllene oxide, Helichrysin, Chlorogenic acid, 6-gingerol, Gallic acid, Catechin, Epigallocatechin, Epicatechin gallate, Nigellidine, and Elacestrant are greater than 0.0, indicating they are highly active.

Jatrorrhizine, Caryophyllene oxide, Spathulenol, 5,7,3',5'-Tetrahydroxyflavanone, Helichrysin, Naringenin, Isoliquiritigen, Cyanidin-3-xyloside, Chlorogenic acid, Ellagic acid, 6-gingerol, Nigellidine, Lignans, Elacestrant, and Fulvestrant have kinase inhibitor properties ranging between -5.0 and 0.0, indicating they are moderately active. Luteolin, Quercetin, Gallic acid, Catechin, Epigallocatechin, Epicatechin, Epicatechin gallate, and Nigellidine have scores greater than 0.0, indicating they are highly active. Nuclear receptor ligand is another predicted bioactivity

score for the compounds of interest. Jatrorrhizine, Spathulenol, Cyanidin-3-xyloside, Nigellidine, and Lignans have nuclear receptor scores between -5.0 and 0.0, suggesting that they are moderately active.

In contrast, Caryophyllene oxide, 5,7,3',5'-Tetrahydroxyflavanone, Helichrysin, Naringenin, Luteolin, Isoliquiritigen, Chlorogenic acid, Quercetin, Ellagic acid, 6-gingerol, Gallic acid, Catechin, Epigallocatechin, Epicatechin, Epicatechin gallate, Nigellidine, Elacestrant, and Fulvestrant have scores greater than 0.0, suggesting that they are highly active.

The protease inhibitor scores for Jatrorrhizine, Caryophyllene oxide, Spathulenol, 5,7,3',5'-Tetrahydroxyflavanone, Helichrysin, Naringenin, Luteolin, Isoliquiritigen, Cyanidin-3-xyloside, Quercetin, Ellagic acid, Nigellidine, and Lignans are between -5.0 and 0.0, indicating that they are moderately active. In contrast, the scores for Chlorogenic acid, Ellagic acid, Gallic acid, Catechin, Epigallocatechin, Epicatechin, Epicatechin gallate, Elacestrant, and Fulvestrant are greater than 0.0, indicating high activity.

The enzyme inhibitor scores for all the compounds Jatrorrhizine, Caryophyllene oxide, Spathulenol, 5,7,3',5'-Tetrahydroxyflavanone, Helichrysin, Naringenin, Luteolin, Isoliquiritigen, Cyanidin-3-xyloside, Chlorogenic acid, Quercetin, Ellagic acid, 6-gingerol, Gallic acid, Catechin, Epigallocatechin, Epicatechin gallate, Nigellidine, Lignans, Elacestrant, and Fulvestrant are all greater than 0.0, indicating high activity.

### ADMET PROPERTIES PREDICTION (PHARMACOKINETICS)

The ADMET analysis of the bioactive compounds alongside control drugs was illustrated in **Table 4**, while **Figures 13-18** illustrate the 3D and 2D interaction of the bioactive compounds in complex with the target protein from the protein plus webserver and Plip. All bioactive compounds that passed molecular docking were further analyzed for pharmacokinetics to evaluate their ADMET (Absorption, Distribution, Metabolism, Excretion, and Toxicity) properties.

In terms of drug absorption, most of the top compounds based on docking scores, along with one control drug, showed low intestinal absorption as measured by Caco-2 permeability, with the exceptions of Helichrysin and Elacestrant. On the other hand, all bioactive compounds and the two control drugs showed greater human intestinal absorption (HIA). Additionally, the ADMET screening results indicated that only the two control drugs and cyanidin-3-xyloside were not substrates for Pgp. All the compounds and reference drugs exhibited increased levels of P-glycoprotein inhibitors (Pgp), except for Caryophyllene oxide and Naringenin. Regarding drug distribution, it was anticipated that all compounds would be able to penetrate

Table 1. Lipinski's drug-likeness virtual screening result of the control drugs and the active compounds using the SwissADME online tool.

S/N	Plant	Molecules	PubChem-ID	Formula	Molecular Weight	XLOGP	Number of Hb Acceptor	Number of HB Donor	Number of Lipinski Violations
1.	<i>Amickia chlorantha</i>	Berberine	2353	C <sub>20</sub> H <sub>18</sub> NO <sub>4</sub> <sup>+</sup>	336.36	3.62	4	0	0
2.		Palmatine	19009	C <sub>21</sub> H <sub>22</sub> NO <sub>4</sub> <sup>+</sup>	352.4	3.75	4	0	0
3.		Jatrorrhizine	72323	C <sub>20</sub> H <sub>20</sub> NO <sub>4</sub> <sup>+</sup>	338.38	3.42	4	11	0
4.		Caryophyllene oxide	1742210	C <sub>15</sub> H <sub>24</sub> O	220.35	3.56	1	0	0
5.		Spathulenol	92231	C <sub>15</sub> H <sub>24</sub> O	220.35	3.11	1	1	0
6.	<i>Cyclopia genistoides</i>	Helichrysin	42607621	C <sub>22</sub> H <sub>24</sub> O <sub>10</sub>	448.42	1.09	10	6	1
7.		Naringenin	439246	C <sub>15</sub> H <sub>12</sub> O <sub>5</sub>	272.25	2.52	5	3	0
8.		5'7'3'5' – tetrahydroxyflavanone	11483087	C <sub>15</sub> H <sub>12</sub> O <sub>6</sub>	C15H12O6	1.52	6	4	0
9.		Luteolin	5280445	C <sub>15</sub> H <sub>10</sub> O <sub>6</sub>	286.24	2.53	6	4	0
10.		Isoliquiritigenin	638278	C <sub>15</sub> H <sub>12</sub> O <sub>4</sub>	256.25	3.18	4	3	0
11.	<i>Allium sativum</i>	Diallyl disulfide	16590	C <sub>6</sub> H <sub>10</sub> S <sub>2</sub>	146.27	2.2	0	0	0
12.		Diallyl trisulfide	16315	C <sub>6</sub> H <sub>10</sub> S <sub>3</sub>	178.34	2.64	0	0	0
13.		Allyl Mercaptan	13367	C <sub>3</sub> H <sub>6</sub> S	74.14	1.16	0	0	0
14.		Gamma-glutamyl-S-2-propenyl	11346811	C <sub>11</sub> H <sub>18</sub> N <sub>2</sub> O <sub>5</sub> S	290.34	-2.84	6	4	0
15.	<i>Rubus fruticosus</i>	Cyanidin-3-rutinoside	441674	C <sub>27</sub> H <sub>31</sub> O <sub>15</sub> <sup>+</sup>	595.53	-2.68	15	10	3
16.		Cyanidin-3-xyloside	71315022	C <sub>20</sub> H <sub>19</sub> ClO <sub>10</sub>	454.81	1.55	10	7	1
17.		Quercetin	5280343	C <sub>15</sub> H <sub>10</sub> O <sup>7</sup>	302.24	1.54	7	5	0
18.		Chlorogenic acid	1794427	C <sub>16</sub> H <sub>18</sub> O <sub>9</sub>	354.31	-0.42	9	6	1
19.		Ellagic acid	5281855	C <sub>14</sub> H <sub>6</sub> O <sub>8</sub>	302.19	1.1	0	8	0
20.	<i>Brassica oleracea</i>	Lutein	5281243	C <sub>40</sub> H <sub>56</sub> O <sub>2</sub>	568.87	11.01	2	2	2
21.		Zeaxanthin	5280899	C <sub>40</sub> H <sub>56</sub> O <sub>2</sub>	568.87	10.91	2	2	2
22.		Indole-3-carbinol	3712	C <sub>9</sub> H <sub>9</sub> N <sub>O</sub>	147.17	1.06	1	2	0
23.		Benzyl Isothiocyanate	2346	C <sub>8</sub> H <sub>7</sub> NS	149.21	3.16	1	0	0
24.		Erucin	78160	C <sub>6</sub> H <sub>11</sub> NS <sub>2</sub>	161.29	2.96	1	0	0

25.	<i>Zingiber officinale</i>	6-gingerol	442793	C <sub>17</sub> H <sub>26</sub> O <sub>4</sub>	294.39	2.76	4	2	0
26.		Paradol	94378	C <sub>17</sub> H <sub>26</sub> O <sub>3</sub>	278.39	4.11	3	1	0
27.		Zingerone	31211	C <sub>11</sub> H <sub>14</sub> O <sub>3</sub>	194.23	1.11	3	1	0
28.		Linalool	6549	C <sub>10</sub> H <sub>18</sub> O	154.25	2.97	1	1	0
29.	<i>Nisella sativa</i>	Thymol	6989	C <sub>10</sub> H <sub>14</sub> O	150.22	3.3	1	1	1
30.		Thymoquinone	10281	C <sub>10</sub> H <sub>12</sub> O <sub>2</sub>	164.2	2.2	2	0	0
31.		Nigellicine	11402337	C <sub>13</sub> H <sub>14</sub> N <sub>2</sub> O <sub>3</sub>	246.26	1.39	3	1	0
32.		Carvacrol	10364	C <sub>10</sub> H <sub>14</sub> O	150.22	3.49	1	1	1
33.		Nigellidine	136828302	C <sub>18</sub> H <sub>18</sub> N <sub>2</sub> O <sup>2</sup>	294.35	2.93	2	1	0
34.	<i>Camellia sinensis</i>	Gallocatechin	65084	C <sub>15</sub> H <sub>14</sub> O <sub>7</sub>	306.27	0	7	6	1
35.		Catechin	9064	C <sub>15</sub> H <sub>14</sub> O <sub>6</sub>	290.27	0.36	6	5	0
36.		Epigallocatechin	72277	C <sub>15</sub> H <sub>14</sub> O <sub>7</sub>	306.27	0	7	6	1
37.		Epicatechin	72276	C <sub>15</sub> H <sub>14</sub> O <sub>6</sub>	290.27	0.36	6	5	0
38.		Epicatechin gallate	107905	C <sub>22</sub> H <sub>18</sub> O <sub>10</sub>	442.37	442.37	10	7	1
39.	<i>Linum usitatissimum</i>	Linamarin	11128	C <sub>10</sub> H <sub>17</sub> NO <sub>6</sub>	247.25	-2.27	7	4	0
40.		Lignans	443013	C <sub>22</sub> H <sub>22</sub> O <sub>8</sub>	414.41	2.01	8	1	0
41.		Linolenic acid	5280934	C <sub>18</sub> H <sub>30</sub> O <sub>2</sub>	278.43	6.46	2	1	1
42.		Amygdalin	656516	C <sub>20</sub> H <sub>27</sub> NO <sub>11</sub>	457.43	-2.71	12	7	2
43.		Lotaustralin	441467	C <sub>11</sub> H <sub>19</sub> NO <sub>6</sub>	261.27	-1.74	7	4	0
44.	Control drugs	Fulvestrant	104741	C <sub>32</sub> H <sub>47</sub> F <sub>5</sub> O <sub>3</sub> S	606.77	9.22	8	2	2
45.		Elacenstrant	23642301	C <sub>30</sub> H <sub>38</sub> N <sub>2</sub> O <sub>2</sub>	458.63	6.3	3	2	1

Table 2. The binding energies and molecular interaction profiles of the control drug and the active compounds.

S/N	Molecule	Binding energies (kcal/mol)	Number of Hydrogen bond (s) formed	Residues involved in hydrogen bond formation (Å)	Residues involved in hydrophobic interaction (Å)	Residues involved in $\pi$ -stacking (Å)	Residues involved in $\pi$ -cation interaction (Å)	Residues involved in Salt Bridge	Residue involved in Halogen
1.	Berberine	-6.2							
2.	Benzyl isothiocyanate	-5.1							
3.	Palmitine	-6.1							
4.	Jatrorrhizine	-6.6							
5.	Caryophyllene Oxide	<b>-8.1*</b>	-		MET343(3.92) TRP383(3.98) HIS524(3.90) LEU525(3.64)				
6.	Spathulenol	<b>-7.9*</b>	-		LEU346(3.82, 3.53) ALA350(3.64)				



				LEU387(3.85)		
				LEU387(3.85)		
				LEU391(3.80)		
				PHE404(3.79)		
				ILE424(3.91)		
				LEU428(3.74)		
				LEU525(3.78)		
7.	5',7',3',5' Tetrahydroxyflavanone	-7.6*	2	GLU353(2.56) LYS449(2.16)	ILE326(3.88, 3.70) ARG394(3.56) PHE445(3.50)	TRP393(4.4 7) ARG394(4.86)
8.	Helichrysin	-7.5*	3	GLU323(2.22) TRP393(2.32) ARG394(4.07)	GLU323(3.89, 3.57)	ARG394(4.85)
9.	Diallyl disulfide	-3.9				
10.	Diallyl trisulfide	-3.8				
11.	Allyl Mercaptan	-2.7				
12.	Gamma-glutamyl-S-2- propenyl	-5.8				
13.	Naringenin	-8.5*	1	GLU353(2.32)	LEU346(3.59) LEU384(3.82) LEU387(3.71) LEU391(3.60) LEU524(3.95)	PHE404(5.0 9)
14.	Luteolin	-8.7*	5	LEU346(1.97) GLU353(2.09) ARG394(3.47) MET528(3.64)	LEU346(3.59) ALA350(3.95) LEU384(3.92) LEU525(3.72)	PHE404(5.1 7)
15.	Isoliquiritigenin	-8.1*	-		LEU349(3.53) ALA350(3.59) LEU387(3.73) PHE404(3.62) LEU525(3.72)	
16.	Cyanidin-3-xyloside	-7*	4	GLU323(2.31) ILE326(3.04) TRP393(3.59) LYS449(1.89)	LEU320(3.46) GLU323(3.46,3.81) ILE326(3.63)	LYS449(4.92 )
17.	Chlorogenic acid	-8.5*	4	THR347(2.60) GLU353(2.24,2 .96) ARG394(3.56)	LEU346(3.56,3.75) ALA350(3.90) LEU384(3.75)	PHE404(5.2 7)
18.	Quercetin	-8.1*	-		LEU346(3.40, 346) ALA350(3.77) LEU525(3.38)	PHE404(5.3 2)
19.	Ellagic acid	-8.4*	2	(LEU2.63) GLU353(2.07)	LEU384(3.94) LEU391(3.91) PHE404(3.44)	
20.	Indole-3-carbinol	-6.2				
21.	Erucin	-2.6				
22.	6-gingerol	-6.4				
23.	Paradol	-6				
24.	Zingerone	-6.2				
25.	Linalool	-5.6				

26	Gallocatechin	-8.2*	4	PRO325(2.29) GLY390(2.37) TRP393(2.39) ARG394(3.08)	GLU323(3.55) PRO324(3.62) ILE326(3.98)	ARG394(4.98)
27	Catechin	-8*	4	GLU353(3.28) GLY390(2.50) TRP393(2.35) ARG394(2.05)	GLU323(3.62) PRO324(3.67) ILE326(3.96)	ARG394(4.98)
28	Epigallocatechin	-8.3*	3	ALA350(3.20) GLU353(2.65) GLY521(2.32)	LEU346(3.38, 3.99) LEU384(3.68) LEU525(3.87, 3.90)	
29	Epicatechin	-8.2*	3	LEU346(2.09) ALA350(3.12) MET528(3.09)	LEU346(3.44) LEU384(3.51) LEU387(3.86) LEU525(3.91, 3.79)	
30	Epicatechin gallate	-7.5*	6	GLU3232(2.38) ILE326(3.16) TRP393(3.20) ARG394(2.78) GLY442(2.39) LYS449(2.38)	GLU323(3.69, 3.86) ILE326(3.95, 3.16) PHE445(4.45) VAL446(4.00)	
31	Thymol	-6				
32	Thymoquinone	-6				
33	Nigellidine	-7.7*	1	THR347(2.46)	LEU346(3.69, 3.72) ALA350(3.78) LEU384(3.93) ILE424(3.61)	
34	Carvacrol	-6.2				
35	Nigellidine	-6.9	2	ILE326(3.20) ARG394(1.92)	LEU320(3.45) GLU323(3.89) ILE326(3.83, 3.77) ARG394(3.84) PHE445(3.71) VAL446(3.72)	TRP393(4.89) GLU323(4.54)
36	Linamarin	-4.7				
37	Lignans	-6.3				
38	Linolenic acid	-5				
39	Lotaustralin	-5.9				
40	Elacestrant	-6.3	9	LEU320(3.47) GLU323(3.88, 3.50) ILE326(3.71, 3.54) TRP393(3.65) PHE445(3.83, 3.63) VAL446(3.93)		
41	Fulvestrant	-6.7	2	ARG394(2.55, 2.45)	GLU323(3.89, 3.59) PRO324(3.62) ILE326(3.85) ARG394(3.87)	GLU353(3.31) LYS449(3.93)

**Table 3. Predicted bioactivity score for bioactive compounds and control drugs**

S/N	Compound name	GPCR ligand	Ion channel modulator	Kinase inhibitor	Nuclear receptor ligand	Protease inhibitor	Enzyme inhibitor
1.	Jatrorrhizine	-0.07	0.82	-0.19	-0.59	-0.30	0.90
2.	Caryophyllene oxide	-0.13	0.14	-0.84	0.45	-0.06	0.42
3.	Spathulenol	-0.42	-0.28	-0.68	-0.28	-0.36	0.06
4.	5,7,3',5'- Tetrahydroxyflavanone	0.06	-0.19	-0.22	0.44	-0.08	0.21
5.	Helichrysin	0.05	0.01	-0.12	0.13	-0.02	0.30
6.	Naringenin	0.03	-0.20	-0.26	0.42	-0.12	0.21
7.	Luteolin	-0.02	-0.07	0.26	0.39	-0.22	0.28
8.	Isoliquiritigenin	-0.13	-0.11	-0.32	0.00	-0.32	0.09
9.	Cyanidin-3- xyloside	-0.02	-0.40	-0.15	-0.24	-0.05	0.07
10.	Chlorogenic acid	0.29	0.14	-0.00	0.74	0.27	0.62
11.	Quercetin	-0.06	-0.19	0.28	0.36	-0.25	0.28
12.	Ellagic acid	-0.29	-0.27	-0.01	0.11	-0.18	0.17
13.	6-gingerol	0.16	0.04	-0.33	0.20	0.15	0.38
14.	Gallocatechin	0.40	0.14	0.14	0.57	0.29	0.49
15.	Catechin	0.41	0.14	0.09	0.60	0.26	0.47
16.	Epigallocatechin	0.40	0.14	0.14	0.57	0.29	0.49
17.	Epicatechin	0.41	0.14	0.09	0.60	0.26	0.47
18.	Epicatechin gallate	0.17	0.02	0.05	0.43	0.13	0.25
19.	Nigellicine	-0.15	-0.00	-0.18	-0.29	-0.57	0.20
20.	Nigellidine	0.07	0.01	0.29	0.10	-0.32	0.19
21.	Lignans	0.14	-0.12	-0.29	-0.09	-0.06	0.18
22.	Elacestrant	0.24	0.09	-0.14	0.13	0.04	0.13
23.	Fulvestrant	0.31	-0.23	-0.31	0.75	0.38	0.43

the blood-brain barrier (BBB). Notably, both Elacestrant and Fulvestrant can cross the blood-brain barrier (BBB). Most of the compounds investigated exhibit a plasma protein binding (PPB) value below 90%, while Helichrysin, Naringenin, Luteolin, Gallocatechin, Catechin, Epigallocatechin, Epicatechin, and Epicatechin gallate, along with Elacestrant and Fulvestrant, have PPB values exceeding 90%. This variation might affect their capacity to target specific sites for pharmacological effects. In terms of drug metabolism, differences were noted in the key enzymes (CYP1A, 2C19, and CYP2C9) related to both inhibitors and substrates across all bioactive compounds and control drugs, suggesting their potential influence on

liver metabolism while functioning as substrates and inhibitors. The assessment of toxicity for the predicted bioactive compounds and reference drugs suggests that only Isoliquiritigenin and Elacestrant exhibit low levels of human hepatotoxicity (H-HT). None of the bioactive compounds assessed were predicted to be toxic to human ether a-go-go (hERG). Four compounds; Caryophyllene oxide, Spathulenol, 5,7,3',5'-Tetrahydroxyflavanone, and Cyanidin-3-xyloside were indicated as potentially carcinogenic substances according to ADMET screening. Notably, none of the control drugs has the potential to cause cancer.

Table 4. Predicted ADMET Properties of Compounds and Control Drug.

S/N	Properties	1. ADMET			2. DISTRIBUTION			3. METABOLISM	
		Caco-2	Pgp-inhibitor	Pgp-Substrate	PPB	BBB	CYP1A2 substrate	CYP1A2 inhibitor	HIA
	Caryophyllene Oxide								
	Spathulenol	No	Yes	No	86.24%	No	No	No	No
	5'7'3'5'	No	No	No	78.72%	No	No	No	No
	Helichrysin	No	No	No	88.90%	No	Yes	No	No
	Naringenin	Yes	No	No	95.59%	No	No	No	No
	Luteolin	No	Yes	No	93.76%	No	Yes	No	No
	Isoliquiritigenin	Yes	No	No	95.44%	No	Yes	No	No
	Cyanidin-3-xyloside	No	No	No	99.19%	No	Yes	No	No
	Chlorogenic acid	Yes	No	Yes	89.78%	No	No	No	No
	Quercetin	Yes	No	No	67.19%	No	Yes	No	No
	Ellagic acid	Yes	No	No	95.50%	No	Yes	No	No
	Gallocatechin	Yes	No	No	78.23%	No	No	No	No
	Catechin	Yes	No	No	91.16%	No	No	No	No
	Epigallocatechin	Yes	No	No	92.06%	No	No	No	No
	Epicatechin	Yes	No	No	91.16%	No	No	No	No
	Epicatechin gallate	Yes	No	No	92.06%	No	No	No	No
	Nigellicine	No	No	No	90.73%	No	No	No	No
	Nigellidine	No	No	No	66.09%	No	No	No	No
	Elaeostrolin	No	No	No	88.60%	No	Yes	No	No
	Fulvestrant	No	No	Yes	96.22%	No	Yes	No	No
	Fulvestrant	Yes	No	Yes	100.39%	No	No	No	No

5. 5. 4.  
TOXICITY EXCRETION

hERG Blockers	$\frac{1}{2}$	CYP3A4 substrate	CYP3A4 inhibitor	CYP2D6 substrate	CYP2D6 inhibitor	CYP2C9 substrate	CYP2C9 inhibitor	CYP2C19 substrate	CYP2C19 inhibitor
No	0.083	No	No	No	No	No	No	Yes	Yes
No	0.064	No	No	No	No	No	No	Yes	No
No	0.875	No	Yes	No	No	No	Yes	No	Yes
No	0.596	No	No	Yes	No	Yes	No	No	No
No	0.774	No	Yes	Yes	No	No	Yes	No	Yes
No	0.898	No	Yes	Yes	Yes	No	No	No	No
No	0.908	No	Yes	Yes	Yes	Yes	Yes	No	Yes
No	0.887	No	No	No	No	No	No	No	No
No	0.928	No	Yes	Yes	No	No	No	No	No
No	0.929	No	No	No	No	Yes	No	No	No
No	0.863	No	No	No	No	No	No	No	No
No	0.870	No	No	No	No	No	No	No	No
No	0.853	No	No	No	No	No	No	No	No
No	0.870	Yes	No	No	No	No	No	No	No
No	0.853	No	No	No	No	No	No	No	No
No	0.923	No	No	No	No	No	No	No	No
No	0.226	No	No	No	No	No	No	No	No
No	0.194	No	Yes	Yes	Yes	Yes	Yes	No	Yes
Yes	0.108	Yes	No	Yes	No	No	No	Yes	No
No	0.012	No	No	No	No	No	No	Yes	Yes



IGC <sub>50</sub>	Carcinogenicity	AMES Toxicity	H-HT
4.373	Yes	No	No
4.079	Yes	No	No
4.700	Yes	No	No
5.049	No	Yes	No
4.992	No	Yes	No
4.432	No	Yes	No
5.205	No	Yes	No
4.541	Yes	Yes	Yes
2.733	No	No	No
4.231	No	Yes	No
3.750	No	Yes	No
3.979	No	Yes	No
4.346	No	Yes	No
3.979	No	Yes	No
4.346	No	Yes	No
4.458	No	No	No
2.681	No	No	No
4.700	No	Yes	No
5.290	No	No	Yes
5.870	No	No	No

## DISCUSSION

Breast cancer encompasses a variety of diseases that initiate in breast tissue, usually manifesting as a lump or mass, with the majority arising from the epithelial cells of the milk ducts. This makes the condition a major health issue, impacting millions of women globally. The need for safer and more effective treatments is crucial, as conventional therapies often lead to significant side effects that can adversely affect patients' quality of life.<sup>56</sup> In this context, medicinal plants present a promising treatment option due to their complex chemical compositions, which may induce apoptosis in cancer cells while sparing healthy tissue.<sup>57</sup> Additionally, the combined effects of different phytochemicals in the selected plants can enhance their efficacy and reduce the risk of drug resistance a frequent problem in standard cancer treatments.<sup>20</sup> Research indicates that the intricate biology of breast cancer involves various genetic and epigenetic alterations that not only encourage tumor proliferation but also offer potential molecular targets for novel therapeutic approaches. It is crucial to utilize these biological targets to design drugs that can effectively interfere with tumor development pathways, thereby improving treatment outcomes for patients with various breast cancer subtypes.<sup>58</sup> Furthermore, creating molecules that support therapeutic interventions is a key focus. In the fast-evolving realm of drug discovery, *in silico* techniques have become essential, providing a more efficient and

cost-effective strategy.<sup>59</sup> These computational methods improve the initial stages of research by aiding in hit selection, lead identification, and optimization, ultimately decreasing both time and cost throughout the drug development process.<sup>60</sup>

This research examined forty-three bioactive compounds derived from nine medicinal plants, targeting the human estrogen receptor alpha (2IOG) to evaluate their potential effects in combating breast cancer. The drug-likeness of the bioactive compounds and control drugs was assessed using Lipinski's rule of five, which evaluates pharmacological properties to determine oral bioavailability via virtual screening. Binding affinities for these compounds were computed and compared to the control drugs, Elacestrant and Fulvestrant, using PyRx software. Furthermore, their ADMET characteristics and biological activity were predicted using online resources. In this study, four out of forty-three bioactive compounds, along with one control drug, failed at least two of Lipinski's five rules following the virtual screening. The compounds Amygdalin, Zeaxanthin, Luteolin, and Cyanidin-3-rutinoside were excluded from further analysis for violating two or more of these rules. Although Fulvestrant also breached two of Lipinski's rules, it was deemed acceptable for further evaluation due to its demonstrated effectiveness against advanced hormone receptor-positive and HER2-negative breast cancer.<sup>61</sup>

In the process of drug discovery, it's important to recognize that the molecular weight of a drug can

impact its efficacy in treating a disease. When the molecular weight exceeds a specific threshold, the compound's surface area increases, leading to a reduced capacity for penetration<sup>50</sup>. As noted by Usha et al. and Singh and Konwar, compounds with a molecular weight exceeding 500 Da, a log P greater than 5, more than 5 hydrogen-bond donors, and over 10 hydrogen-bond acceptors are generally considered unsuitable for oral medication because they may lack essential properties related to absorption, distribution, metabolism, and excretion<sup>62,63</sup>. This finding suggests that the bioactive compounds that complied with Lipinski's rules of five demonstrate good drug characteristics and show potential for use as oral drugs.

Molecular docking has become an effective computational method for evaluating the interactions between a protein and a ligand, allowing predictions of the ligand's binding affinity and activity. This method helps identify the best conformation of the ligand about the macromolecular target, like an enzyme or receptor, allowing for the formation of a stable complex<sup>64</sup>. It employs binding free energy, an important thermodynamic factor, to evaluate the theoretical stability of the ligand-protein complex<sup>62,65</sup>. The molecular docking analysis conducted in this research revealed that Luteolin obtained from *Cyclopia genistoides*, had the strongest binding energy among all the evaluated bioactive compounds when compared to other ligands and the reference drugs (**Table 2**). Luteolin showed a binding energy of -8.7 kcal/mol, while Chlorogenic acid and Naringenin, derived from *Cyclopia genistoides* and *Rubus fruticosus* respectively, both exhibited binding energies of -8.5 kcal/mol. Subsequently, Ellagic acid derived from *Rubus fruticosus* had a binding energy of -8.4 kcal/mol. Compounds including Epigallocatechin, Epicatechin, Gallic acid, Isoliquiritigenin, Caryophyllene oxide, Quercetin, Catechin, Spathulenol, Nigellidine, 5'7'3'5'-tetrahydroxyflavanone, Helichrysin, Epicatechin gallate, Cyanidin-3-xyloside, and Nigellidine exhibited binding energies of (-8.3 -8.2, -8.1, -8.1 -8.0 -7.9, -7.7, -7.6, -7.5, -7.5, -7.0 and -6.9) kcal/mol, respectively. All these binding interactions were stronger than those of the control drugs, which exhibited binding energies of (-6.3 and -6.7) kcal/mol for Elacestrant and Fulvestrant, respectively. The study predicts binding conformations based on the shape and electrostatic interactions of the ligands and proteins, which can be quantified. The total interactions are estimated to represent the ligand's docking score in the protein's binding pocket, expressed as a negative energy value in kcal/mol. A lower negative total energy indicates a stronger binding interaction. The docking method accurately predicts the optimal binding of compounds within the protein's active site, revealing that Luteolin, Chlorogenic acid, and Naringenin have a more robust interaction with the target protein, potentially inhibiting effects caused by the Human

estrogen receptor alpha. The higher binding scores of the compounds suggested that they interact more strongly with the estrogen receptor than Fulvestrant and Elacestrant. This could imply that these bioactive compounds might be more effective in altering the receptor's activity. Although Fulvestrant and Elacestrant are specifically designed to function as estrogen receptor antagonists, the natural compounds may serve dual purposes, possibly functioning as agonists or antagonists based on the cellular environment.

The interaction of bioactive compounds with the Human estrogen receptor  $\alpha$  (ER $\alpha$ ) may offer anti-cancer benefits in breast cancer therapy by blocking the protein target. Additionally, these compounds show promise in binding to the receptor's catalytic sites. The interaction between compound 11F and the ligand-binding domain of the estrogen receptor alpha (ER $\alpha$ ) involves various molecular interactions, including hydrophobic interactions, hydrogen bonds,  $\pi$ -stacking, and salt bridges. The presence of hydrogen bonding and hydrophobic interactions may affect the structure and function of the protease, playing an essential role in stabilizing the complex conformation.<sup>65</sup> The ligand 11F forms hydrophobic interactions with the hydrophobic pocket of the ER $\alpha$ , which helps it to fit stably into the binding site. Additionally, the presence of polar functional groups like hydroxyl (-OH) or carbonyl (C=O) facilitates the formation of hydrogen bonds with important amino acid residues, which increases binding affinity and helps stabilize the complex. Furthermore, the protein exhibits strong van der Waals forces due to the close distance of 11F to the binding site, enhancing the total binding energy. The attachment of 11F also leads to notable conformational alterations in ER $\alpha$ .<sup>51,55,65</sup>

As seen in the stronger binding energies of Luteolin, Chlorogenic acid, and Naringenin exhibit stronger interaction with ER $\alpha$  than Elacestrant and Fulvestrant, suggesting their potential as effective inhibitors of this receptor and as candidates for breast cancer therapies. Luteolin with the highest docking score of -8.7 kcal/mol, engaging with amino acid residues LEU346, GLU353, ARG394, GLY521, and MET528 via hydrogen bonds, hydrophobic interactions with LEU346, ALA350, LEU384, and LEU525, and  $\pi$ -stacking with PHE404 (**Figure 14d**). Chlorogenic acid binds with residues THR347, GLU353, and ARG394 through hydrogen bonds, while also interacting hydrophobically with LEU346, ALA350, and LEU384, and exhibiting  $\pi$ -stacking with PHE404 (**Figure 15b**). Naringenin interacts hydrophobically with LEU346, LEU384, LEU387, LEU391, and LEU525, and shows favorable binding at GLU353 and PHE404 through hydrogen bonds and  $\pi$ -stacking, respectively (**Figure 14b**). Ellagic acid, also from *Rubus fruticosus*, binds to LEU346 and GLU353 using hydrogen bonds and exhibits three hydrophobic interactions with LEU384, LEU391, and PHE404 (**Figure 15d**). Consequently, the

compounds Luteolin, Chlorogenic acid, and Naringenin are likely to exhibit great effectiveness against the human estrogen receptor  $\alpha$  compared to the control drugs Elacestrant and Fulvestrant, due to their higher binding energies and interaction with the target protein. The binding interactions of Luteolin, Chlorogenic acid, and Naringenin with 2IOG have been found to obstruct the entry of additional substrates, potentially limiting cancer cell proliferation associated with breast cancer and alleviating negative effects prompted by estrogen receptor  $\alpha$ . Thus, the attachment of these bioactive compounds to the 2IOG protein could offer anti-breast cancer benefits by inhibiting this target, highlighting their potential to engage with the catalytic sites of the target.

Assessing the bioactivity of chemical compounds is a vital part of the drug discovery process, as it allows researchers to pinpoint promising candidates for additional study. A widely used method is to implement bioactivity scoring systems that allocate numerical scores to indicate the possible biological activity of a compound. Overall, compounds or ligands that have a bioactivity score greater than 0.00 are regarded as having significant biological activity. In contrast, scores ranging from -5.0 to 0.00 are seen as indicative of moderate activity, whereas scores lower than -5.0 imply that the molecules are inactive.<sup>66</sup> **Table 3** presents the bioactivity scores for the compounds, which were obtained using the Molinspiration web server tool. This study's findings indicate that the bioactive compounds, Chlorogenic acid, Gallic acid, Catechin, Epigallocatechin, Epicatechin, and Epicatechin gallate exhibit strong bioactivity scores above -0.00, highlighting their high activity against protein targets in comparison to other tested ligands. To be considered a viable drug candidate for clinical trials, a compound must have a favorable pharmacokinetic profile, a substantial safety margin, and a lower chance of toxicity and negative side effects. In comparison, Jatrorrhizine, Caryophyllene oxide, Spathulenol, 5,7,3',5'-tetrahydroxyflavanone, Helichrysin, Naringenin, Luteolin, Isoliquiritigenin, Cyanidin-3-xyloside, Quercetin, Ellagic acid, 6-gingerol, Nigellidine, Nigellidine, Lignans, and the control drugs are considered to have moderate activity, as their bioactivity scores range from -5.0 to 0.00. To be considered a viable drug candidate for clinical trials, a compound needs to have a suitable pharmacokinetic profile, a significant safety buffer, and a lower risk of toxicity and side effects.

In the development of novel pharmaceutical compounds, it is crucial to comprehend their absorption, distribution, metabolism, excretion, and toxicity properties. To assess the pharmacological characteristics of several bioactive compounds, an analysis of their ADMET profiles was conducted using the online platform ADMETlab. The properties offer valuable

information regarding the pharmacological characteristics of the compounds and their ability to reach their target protein.<sup>67</sup> The ADMET properties of both the control drugs and the screened ligands are presented in **Table 4**. Compounds with higher docking scores than the control drugs were exempted from ADMET screening.

A key challenge for oral drugs is their ability to traverse the intestinal epithelial barrier, which influences the rate and extent of absorption in the human body, ultimately impacting their bioavailability.<sup>68</sup> Therefore, Human Intestinal Absorption (HIA) and Caco-2 were chosen to assess the absorption properties. As illustrated in **Table 4**, only one of the hit compounds and control drug demonstrated a higher caco-2- permeability value, and none of the bioactive compounds showed a lower HIA value. According to Puri *et al.*, P-glycoprotein is a critical ATP-binding cassette protein involved in effluxing molecules from cells, preventing compounds from bioaccumulating, and modulating their pharmacological response. In this context, the models of P-glycoprotein inhibition or substrate were utilized as a crucial criterion for assessing the drugs from this perspective. All the hit compounds were identified as inhibitors of P-glycoprotein and Pgp substrate, while Elacestrant and Fulvestrant were not Pgp substrates. This suggests that they may possess a significant implication for their pharmacokinetics and may be effective for administration.<sup>68,69</sup>

Plasma protein binding is an essential mechanism governing drug uptake and distribution. The pharmacodynamic characteristics of drugs are influenced by their ability to bind to plasma proteins<sup>70</sup>. The oral bioavailability of a drug can be influenced by plasma protein binding (PPB), when a drug attaches to serum proteins during this process, its free concentration is compromised. A drug is regarded as having appropriate PPB if its predicted value is below 90%, and drugs with high protein binding may exhibit a narrow therapeutic index<sup>71,72</sup>. However, most of the hit compounds in our study show the value of plasma protein binding (PPB) greater than 90%. This variation could influence their ability to reach target sites for pharmacological effects. The ability of bioactive compounds to cross the blood-brain barrier (BBB) indicates their potential to serve as a therapeutic drug and the findings of these studies reveal that all the compounds and reference drugs were expected to cross the blood-brain barrier (BBB). This suggests that these compounds could effectively reach central nervous system (CNS) targets, positioning them as promising candidates for further development in drug discovery.

The CYP enzymes, especially the isoforms 1A2, 2C9, 2C19, 2D6 and 3A4, account for approximately 90% of oxidative metabolic reactions<sup>73</sup>. The potential of a small molecule to inhibit a greater number of CYP isoforms increases its likelihood of

participating in drug-drug interactions (DDI) with various other drugs.<sup>74</sup> Catechin and epicatechin gallate do not inhibit any CYP isoforms, suggesting a positive metabolic profile with a low risk of drug-drug interactions mediated by CYP enzymes. This characteristic increases their attractiveness in drug discovery and development because it enables safer and more predictable pharmacokinetics, while also minimizing worries about negative interactions with other drugs. **Table 4** shows that Gallocatechin and Epicatechin do not inhibit the majority of CYP isoforms, indicating they possess a beneficial metabolic profile with a low likelihood of interactions involving most CYP enzymes. The ADMET results presented in **Table 4** indicate that Helichrysin, Epigallocatechin, Chlorogenic acid, Luteolin, and Naringenin selectively inhibit various CYP isoforms, implying a moderate risk of drug-drug interactions (DDIs) based on their metabolic pathways. This selective inhibition highlights their relative safety while emphasizing the need to monitor possible interactions with drugs that are metabolized by these specific CYPs throughout the drug discovery process. The toxicity properties addressed several key endpoints, such as AMES toxicity, Ototoxicity, CARC, and hERG among others. The blockage of the hERG potassium channel can lead to prolonged QT intervals, potentially leading to serious cardiac issues, which poses a significant challenge in the clinical evaluation of drug candidates.<sup>75</sup> Therefore, incorporating the hERG model into this scoring function is essential. It's worth mentioning that among all the assessed ligands and control drugs, only the control drug, Elacestrant exhibits a low hERG blocker value. This indicates that these compounds with optimal hERG values show great potential for future advancements, as they present a low risk of cardiotoxicity.

Furthermore, carcinogenicity is a critical toxicological endpoint that raises significant concerns for human health. Many drugs, including canrenone and hexestrol, have been taken off the market due to their carcinogenic effects. We have chosen the most relevant endpoints to develop the ADMET-score function<sup>76</sup>. ADMET analysis shows that Caryophyllene oxide, Spathulenol, 5,7,3',5'-tetrahydroxyflavanone, and Cyanidin-3-xyloside may have carcinogenic potential, with scores exceeding -0.7. Conversely, all identified compounds and control medications exhibit no risk of carcinogenicity. Their positive safety profile positions them as promising options for pharmacokinetic research and future therapeutic use.

Most of the compounds with docking scores between -7.0 kcal/mol and -8.7 kcal/mol exhibit ADMET properties that were better than the control drugs, though there is a need for molecular simulation and pharmacophore modeling, which can improve some of the fundamental ADMET properties of the ligands.

## CONCLUSION

Our findings indicated that four of these compounds did not adhere to at least two of Lipinski's Rule of 5. Moreover, 21 out of the remaining 39 compounds exhibited binding energies that surpassed those of the control drugs Fulvestrant and Elacestrant. Additionally, compounds such as Helichrysin, Epicatechin gallate, Catechin, Epicatechin, Gallocatechin, Epigallocatechin, Chlorogenic acid, Naringenin, and Luteolin, showed favorable binding energies derived from *Cyclopia genistoides*, *Rubus fruticosus*, and *Camellia sinensis*, demonstrated superior binding energies to 2IOG compared to the control drugs. These compounds also displayed favorable bioactivity scores and ADMET properties, indicating their potential as active and effective inhibitors for breast cancer receptor therapies. Further biological activity assessments and laboratory experiments such as molecular dynamics simulation, in-vivo and in-vitro are suggested to confirm the computational findings and to aid in the development of new breast cancer treatments.

## Funding

This research did not receive any specific grant from funding agencies in the public, commercial, or not-for-profit sectors.

## Conflict of interest

The authors declare that there isn't any conflict of interest regarding the publication of this paper.

## Acknowledgment

All authors acknowledge their respective institutions for providing the enabling environment to carry out this work.

## REFERENCES

1. Ahmad S, Shaukat MT, Rehman WU, Mohsin A, Rehman AU, Graff SL. The global and regional disease burden of breast cancer from 1980 to 2021: An analysis of GBD study 2021. *JCO Oncol Pract.* **2024**;20(10\_suppl):146-146. doi: 10.1200/OP.2024.20.10\_suppl.146
2. Arnold M, Morgan E, Rungay H, et al. Current and future burden of breast cancer: Global statistics for 2020 and 2040. *The Breast.* **2022**; 66:15-23. doi: 10.1016/j.breast.2022.08.010
3. Fu J, Zhou B, Zhang L, et al. Expressions and significances of the angiotensin-converting enzyme 2 gene, the receptor of SARS-CoV-2 for COVID-19. *Mol Biol Rep.* **2020**;47(6):4383-4392. doi:10.1007/s11033-020-05478-4



4. Benson JR, Jatoi I. The Global Breast Cancer Burden. *Future Oncol.* **2012**;8(6):697-702. doi:10.2217/fon.12.61
5. Jemal A, Bray F, Center MM, Ferlay J, Ward E, Forman D. Global cancer statistics. *CA: A Cancer Journal for Clinicians.* **2011**;61(2):69-90. doi:10.3322/caac.20107
6. Siegel R, Naishadham D, Jemal A. Cancer statistics, **2013**. *CA A Cancer J Clinicians.* 2013;63(1):11-30. doi:10.3322/caac.21166
7. Patani N, Martin L, Dowsett M. Biomarkers for the clinical management of breast cancer: International perspective. *Intl Journal of Cancer.* **2013**;133(1):1-13. doi:10.1002/ijc.27997
8. Thomas C, Gustafsson JÅ. The different roles of ER subtypes in cancer biology and therapy. *Nat Rev Cancer.* **2011**;11(8):597-608. doi:10.1038/nrc3093
9. Omoto Y, Iwase H. Clinical significance of estrogen receptor  $\beta$  in breast and prostate cancer from biological aspects. *Cancer Science.* **2015**;106(4):337-343. doi:10.1111/cas.12613
10. Lee N, Park MJ, Song W, Jeon K, Jeong S. Currently Applied Molecular Assays for Identifying ESR1 Mutations in Patients with Advanced Breast Cancer. *IJMS.* **2020** ;21(22):8807. doi :10.3390/ijms21228807
11. Lu Y, Gutgesell LM, Xiong R, et al. Design and Synthesis of Basic Selective Estrogen Receptor Degradable for Endocrine Therapy Resistant Breast Cancer. *J Med Chem.* **2019**;62(24):11301-11323. doi: 10.1021/acs.jmedchem.9b01580
12. Alvarez R. Present and future evolution of advanced breast cancer therapy. *Breast cancer research: BCR.* **2010**;12 Suppl 2:S1. doi:10.1186/bcr2572
13. Hageman E, Lussier ME. Elacestrant for ER-Positive HER2-Negative Advanced Breast Cancer. *Ann Pharmacother.* **2024**;58(8):849-856. doi:10.1177/10600280231206131
14. Boér K. Fulvestrant in advanced breast cancer: evidence to date and place in therapy. *Ther Adv Med Oncol.* **2017**;9(7):465-479. doi:10.1177/1758834017711097
15. Kalinsky K, Bianchini G, Hamilton EP, et al. Abemaciclib plus fulvestrant vs fulvestrant alone for HR+, HER2- advanced breast cancer following progression on a prior CDK4/6 inhibitor plus endocrine therapy: Primary outcome of the phase 3 postMONARCH trial. *JCO.* **2024**;42(17\_suppl):LBA1001-LBA1001. doi: 10.1200/JCO.2024.42.17\_suppl.LBA1001
16. Traditional medicine. Accessed August 14, **2024**. <https://www.who.int/news-room/questions-and-answers/item/traditional-medicine>
17. Choudhari AS, Mandave PC, Deshpande M, Ranjekar P, Prakash O. Phytochemicals in Cancer Treatment: From Preclinical Studies to Clinical Practice. *Front Pharmacol.* **2020**; 10:1614. doi:10.3389/fphar.2019.01614
18. Barnum CR, Endelman BJ, Shih PM. Utilizing Plant Synthetic Biology to Improve Human Health and Wellness. *Front Plant Sci.* **2021**; 12:691462. doi:10.3389/fpls.2021.691462
19. Chota A, P. George B, Abrahamse H. Plant-Derived Anticancer Compounds Used in Cancer Therapies. In: Atta-ur-Rahman, Choudhary MI, eds. *Frontiers in Natural Product Chemistry.* Vol 7. BENTHAM SCIENCE PUBLISHERS; **2021**:1-30. doi:10.2174/9781681089164121070003
20. Assob JCN, Nsagha DS, Ngum NM, Kuete V. Toxicological Societies in Africa. In: *Toxicological Survey of African Medicinal Plants.* Elsevier; **2014**:1-15. doi:10.1016/B978-0-12-800018-2.00001-7
21. Akinwale SG, Chukwu OE, Chioma OP, Chukudi AJ, Olubunmi AG. Enantia chlorantha: A review. *J Pharmacogn Phytochem.* **2022**;11(3):34-38. doi: 10.22271/phyto.2022.v11.i3a.14406
22. Davares AKL, Arsene MMJ, Viktorovna PI, Shommya D. Enantia chlorantha and its Multiple Therapeutic Virtues: A Mini Review. *JPRI.* Published online September 30, **2021**:254-259. doi:10.9734/jpri/2021/v33i45A32741
23. Patiño-Morales CC, Jaime-Cruz R, Sánchez-Gómez C, et al. Antitumor Effects of Natural Compounds Derived from Allium sativum on Neuroblastoma: An Overview. *Antioxidants.* **2021**;11(1):48. doi:10.3390/antiox11010048
24. White D. Healthy Uses for Garlic. *Nursing Clinics of North America.* **2021**;56(1):153-156. doi: 10.1016/j.cnur.2020.12.001
25. Benavides GA, Squadrito GL, Mills RW, et al. Hydrogen sulfide mediates the vasoactivity of garlic. *Proc Natl Acad Sci USA.* **2007**;104(46):17977-17982. doi:10.1073/pnas.0705710104
26. Sharma JR, Sibuyi NRS, Fadaka AO, et al. Anticancer and Drug-Sensitizing Activities of Gold Nanoparticles Synthesized from Cyclopia genistoides (Honeybush) Extracts. *Applied Sciences.* **2023**;13(6):3973. doi:10.3390/app13063973
27. Trio PZ, You S, He X, He J, Sakao K, Hou DX. Chemopreventive functions and molecular mechanisms of garlic organosulfur compounds. *Food Funct.* **2014**;5(5):833. doi:10.1039/c3fo60479a
28. Wang M, Lai X, Shao L, Li L. Evaluation of immunoresponses and cytotoxicity from skin exposure to metallic nanoparticles. *IJN.* **2018**; 13:4445-4459. doi:10.2147/IJN.S170745
29. Murakami S, Miura Y, Hattori M, et al. Cyclopia Extracts Enhance Th1-, Th2-, and Th17-type T Cell Responses and Induce Foxp3+ Cells in Murine Cell



- Culture. *Planta Med.* **2018**;84(05):311-319. doi:10.1055/s-0043-121270
30. Verma R, Gangrade T, Ghulaxe C, Punasiya R. Rubus fruticosus (blackberry) use as an herbal medicine. *Phcog Rev.* **2014**;8(16):101. doi:10.4103/0973-7847.134239
31. Šamec D, Salopek-Sondi B. Cruciferous (Brassicaceae) Vegetables. In: *Nonvitamin and Nonmineral Nutritional Supplements*. Elsevier; **2019**:195-202. doi:10.1016/B978-0-12-812491-8.00027-8
32. Franzke A, Lysak MA, Al-Shehbaz IA, Koch MA, Mummenhoff K. Cabbage family affairs: the evolutionary history of Brassicaceae. *Trends in Plant Science.* **2011**;16(2):108-116. doi: 10.1016/j.tplants.2010.11.005
33. Umesh CV. Camellia sinensis. In: *Herbs, Spices and Their Roles in Nutraceuticals and Functional Foods*. Elsevier; **2023**:219-231. doi :10.1016/B978-0-323-90794-1.00009-0
34. Hannan MdA, Rahman MdA, Sohag AAM, et al. Black Cumin (*Nigella sativa* L.): A Comprehensive Review on Phytochemistry, Health Benefits, Molecular Pharmacology, and Safety. *Nutrients.* **2021**;13(6):1784. doi:10.3390/nu13061784
35. Zadorozhna M, Mangieri D. Mechanisms of Chemopreventive and Therapeutic Proprieties of Ginger Extracts in Cancer. *IJMS.* **2021**;22(12):6599. doi:10.3390/ijms22126599
36. Lee H, Seo E, Kang N, Kim W. [6]-Gingerol inhibits metastasis of MDA-MB-231 human breast cancer cells. *The Journal of Nutritional Biochemistry.* **2008**;19(5):313-319. doi: 10.1016/j.jnutbio.2007.05.008
37. Parikh M, Netticadan T, Pierce GN. Flaxseed: its bioactive components and their cardiovascular benefits. *American Journal of Physiology-Heart and Circulatory Physiology.* **2018**;314(2):H146-H159. doi:10.1152/ajpheart.00400.2017
38. Qamar H. Flax: Ancient to modern food. *PAB.* **2019** ;8(4). doi :10.19045/bspab.2019.80173
39. Dai SX, Li WX, Han FF, et al. In silico identification of anti-cancer compounds and plants from traditional Chinese medicine database. *Sci Rep.* **2016**;6(1):25462. doi:10.1038/srep25462
40. Akinwumi I, Faleti A, Owojuyigbe A, Raji F, Alaka M. In Silico Studies of Bioactive Compounds Selected from Four African Plants with Inhibitory Activity Against Plasmodium falciparum Dihydrofolate Reductase-Thymidylate Synthase (pfDHFR-TS). *Journal of Advanced Pharmacy Research.* **2022**;6(3):107-122. doi:10.21608/aprh.2022.139794.1175
41. Akinwumi IA, Ishola BO, Adeyemo OM, Owojuyigbe AP. Evaluation of therapeutic potentials of some bioactive compounds in selected African plants targeting main protease (Mpro) in SARS-CoV-2: a molecular docking study. *Egypt J Med Hum Genet.* **2023**;24(1):80. doi:10.1186/s43042-023-00456-4
42. Oladele T, Bewaji C, Sadiku J. Drug target selection for malaria: Molecular basis for the drug discovery process. *Centrepont Journal.* **2012**; 00:111-124.
43. Sarbadhikary P, George BP. A Review on Traditionally Used African Medicinal Plant *Annickia chlorantha*, Its Phytochemistry, and Anticancer Potential. *Plants.* **2022**;11(17):2293. doi:10.3390/plants11172293
44. Esghaei M, Ghaffari H, Rahimi Esboei B, Ebrahimi Tapeh Z, Bokharaei-Salim F, Motevalian M. Evaluation of Anticancer Activity of *Camellia Sinensis* in the Caco-2 Colorectal Cancer Cell Line. *Asian Pac J Cancer Prev.* **2018**;19(6). doi:10.22034/APJCP.2018.19.6.1697
45. Kim S, Chen J, Cheng T, et al. PubChem 2023 update. *Nucleic Acids Research.* **2023** ;51(D1): D1373-D1380. doi:10.1093/nar/gkac956
46. Dykstra KD, Guo L, Birzin ET, et al. Estrogen receptor ligands. Part 16: 2-Aryl indoles as highly subtype selective ligands for ER $\alpha$ . *Bioorganic & Medicinal Chemistry Letters.* **2007**;17(8):2322-2328. doi: 10.1016/j.bmcl.2007.01.054
47. Bank RPD. RCSB PDB. Accessed August 14, 2024. <https://www.rcsb.org/search>
48. Pettersen EF, Goddard TD, Huang CC, et al. UCSF Chimera—A visualization system for exploratory research and analysis. *J Comput Chem.* **2004**;25(13):1605-1612. doi:10.1002/jcc.20084
49. Daina A, Michielin O, Zoete V. SwissADME: a free web tool to evaluate pharmacokinetics, drug-likeness and medicinal chemistry friendliness of small molecules. *Sci Rep.* **2017**;7(1):42717. doi:10.1038/srep42717
50. Lipinski CA. Rule of five in 2015 and beyond: Target and ligand structural limitations, ligand chemistry structure and drug discovery project decisions. *Advanced Drug Delivery Reviews.* **2016**; 101:34-41. doi: 10.1016/j.addr.2016.04.029
51. Suganya J, Radha M, Naorem DL, Nishandhini M. In Silico Docking Studies of Selected Flavonoids - Natural Healing Agents against Breast Cancer. *Asian Pacific Journal of Cancer Prevention.* **2014**;15(19):8155-8159. doi:10.7314/APJCP.2014.15.19.8155
52. Trott O, Olson AJ. AutoDock Vina: improving the speed and accuracy of docking with a new scoring function, efficient optimization, and multithreading. *J Comput Chem.* **2010**;31(2):455-461. doi:10.1002/jcc.21334
53. Calculation of molecular properties and bioactivity score. Accessed October 19, **2024**. <https://molinspiration.com/cgi/properties>
54. Xiong G, Wu Z, Yi J, et al. ADMETlab 2.0: an integrated online platform for accurate and

- comprehensive predictions of ADMET properties. *Nucleic Acids Research*. **2021**;49(W1): W5-W14. doi:10.1093/nar/gkab255
55. Roy A, Anand A, Garg S, et al. Structure-Based in Silico Investigation of Agonists for Proteins Involved in Breast Cancer. Garg R, ed. *Evidence-Based Complementary and Alternative Medicine*. **2022**; 2022:1-12. doi:10.1155/2022/7278731
56. Li YX, Himaya SWA, Dewapriya P, Zhang C, Kim SK. Fumigaclavine C from a Marine-Derived Fungus *Aspergillus Fumigatus* Induces Apoptosis in MCF-7 Breast Cancer Cells. *Marine Drugs*. **2013**;11(12):5063-5086. doi:10.3390/md11125063
57. Harnessing Nature's Power: A Comprehensive Review of Indian Plant Extracts in Cancer Therapy. Pure Natural Plant Extracts Manufacturer - Over 19 Years. Accessed August 19, **2024**. [https://www.greenskybio.com/plant\\_extract/harnessing-natures-power-a-comprehensive-review-of-indian-plant-extracts-in-cancer-therapy.html](https://www.greenskybio.com/plant_extract/harnessing-natures-power-a-comprehensive-review-of-indian-plant-extracts-in-cancer-therapy.html)
58. Viale G, Bottiglieri L. Pathological definition of triple negative breast cancer. *European Journal of Cancer*. **2009**; 45:5-10. doi:10.1016/S0959-8049(09)70011-5
59. Issa N, Byers S, Dakshanamurthy S. Drug Repurposing: Translational Pharmacology, Chemistry, Computers and the Clinic. *CTMC*. **2013**;13(18):2328-2336. doi:10.2174/15680266113136660163
60. Bauer J, Rajagopal N, Gupta P, Gupta P, Nixon AE, Kumar S. How can we discover developable biotherapeutics? *Front Mol Biosci*. **2023**; 10:1221626. doi:10.3389/fmolb.2023.1221626
61. FDA Expands Approval of Fulvestrant for Breast Cancer - NCI. September 22, 2017. Accessed October 21, **2024**. <https://www.cancer.gov/news-events/cancer-currents-blog/2017/fda-fulvestrant-breast-cancer>
62. Usha T, Middha SK, Goyal AK, et al. Molecular docking studies of anti-cancerous candidates in *Hippophae rhamnoides* and *Hippophae salicifolia*. *J Biomed Res*. **2014**; 28(5):406-415. doi:10.7555/JBR.28.20130110
63. Singh SP, Konwar BK. Molecular docking studies of quercetin and its analogues against human inducible nitric oxide synthase. *Springerplus*. **2012**; 1(1):69. doi:10.1186/2193-1801-1-69
64. MDM2 case study: Computational protocol utilizing protein flexibility and data mining improves ligand binding mode predictions. *bioRxiv*. Published online January 1, **2016**: 054239. doi:10.1101/054239
65. El Khatabi K, Aanouz I, Alaqarbeh M, Ajana MA, Lakhlifi T, Bouachrine M. Molecular docking, molecular dynamics simulation, and ADMET analysis of levamisole derivatives against the SARS-CoV-2 main protease (M<sup>Pro</sup>). *Bioimpacts*. **2021** ;12(2) :107-113. doi :10.34172/bi.2021.22143
66. Qureshi R, Irfan M, Gondal TM, et al. AI in drug discovery and its clinical relevance. *Heliyon*. **2023**; 9(7): e17575. doi: 10.1016/j.heliyon. 2023.e17575
67. Sharma A, Sharma S, Gupta M, Fatima S, Saini R, Agarwal SM. Pharmacokinetic profiling of anticancer phytochemicals using computational approach. *Phytochemical Analysis*. **2018** ; 29(6):559-568. doi :10.1002/pca.2767
68. Guan L, Yang H, Cai Y, et al. ADMET-score – a comprehensive scoring function for evaluation of chemical drug-likeness. *Med Chem Commun*. **2019**; 10(1):148-157. doi:10.1039/C8MD00472B
69. Moon A, Khan D, Gajbhiye P, Jariya M. Insilico prediction of toxicity of ligands utilizing admetstar. *Int J Pharm Bio Sci*. **2017**; 8(3). doi:10.22376/ijpbs.2017.8.3. b674-677
70. Puri S, Ahmad I, Patel H, Kumar K, Juvale K. Evaluation of oxindole derivatives as a potential anticancer agent against breast carcinoma cells: In vitro, in silico, and molecular docking study. *Toxicology in Vitro*. **2023**; 86:105517. doi: 10.1016/j.tiv.2022.105517
71. Akinwumi IA, Ishola B, Musbau R, Abubakar A, Owojuyigbe A. Therapeutic Potential and Molecular Docking Perspective of Six Medicinal Plants against the Human SIRT-6 Protein Implicated in Type-2 Diabetes. *Journal of Advanced Pharmacy Research*. **2023**;7(4):205-231. doi:10.21608/aprh.2023.222618.1226
72. Brogi S, Ramalho TC, Kuca K, Medina-Franco JL, Valko M. Editorial: In silico Methods for Drug Design and Discovery. *Front Chem*. **2020**; 8:612. doi:10.3389/fchem.2020.00612
73. Wei Y, Palazzolo L, Ben Mariem O, et al. Investigation of in silico studies for cytochrome P450 isoforms specificity. *Computational and Structural Biotechnology Journal*. **2024**; 23:3090-3103. doi: 10.1016/j.csbj.2024.08.002
74. Cheng F, Yu Y, Zhou Y, et al. Insights into Molecular Basis of Cytochrome P450 Inhibitory Promiscuity of Compounds. *J Chem Inf Model*. **2011**; 51(10) :2482-2495. doi :10.1021/ci200317s
75. Liao J, Yang Z, Yang J, et al. Investigating the cardiotoxicity of N-n-butyl haloperidol iodide: Inhibition mechanisms on hERG channels. *Toxicology*. **2024**; 508:153916. doi: 10.1016/j.tox.2024.153916
76. Siramshetty VB, Nickel J, Omieczynski C, Gohlke BO, Drwal MN, Preissner R. WITHDRAWN—a resource for withdrawn and discontinued drugs. *Nucleic Acids Res*. **2016**; 44(D1): D1080-D1086. doi:10.1093/nar/gkv1192